msp

Algebraic & Geometric Topology 18 (2018) 1411–1459

A colored Khovanov spectrum and its tail for B–adequate links

MICHAEL WILLIS

We define a Khovanov spectrum for $\mathfrak{sl}_2(\mathbb{C})$–colored links and quantum spin networks and derive some of its basic properties. In the case of n–colored B–adequate links, we show a stabilization of the spectra as the coloring $n \to \infty$, generalizing the tail behavior of the colored Jones polynomial. Finally, we also provide an alternative, simpler stabilization in the case of the colored unknot.

57M27, 57M25

1 Introduction

In [5], Mikhail Khovanov introduced the Khovanov homology $\mathrm{Kh}^{i,j}(L)$ of a knot or link L, the homology of a bigraded chain complex $\mathrm{KC}^{i,j}(L)$ with graded Euler characteristic equal to the Jones polynomial of L. In [7], Robert Lipshitz and Sucharit Sarkar defined the Khovanov spectrum of L, a wedge sum of spectra $\mathcal{X}^j(L)$ whose reduced cohomology groups satisfy $\widetilde{H}^i(\mathcal{X}^j(L)) \cong \mathrm{Kh}^{i,j}(L)$. It is then natural to ask what types of structural results about Khovanov homology extend to the Khovanov spectrum.

In [16], the author proved that for the torus links $T(n,m)$, the Khovanov spectra $\mathcal{X}(T(n,m))$ stabilize as $m \to \infty$, allowing a well-defined notion of a limiting Khovanov spectrum $\mathcal{X}(T(n,\infty))$. Due to Lev Rozansky's arguments in [12], this result could be interpreted as defining a colored Khovanov spectrum for the n–colored unknot. (Here "colored" refers to assigning an irreducible $\mathfrak{sl}_2(\mathbb{C})$ representation to each component of the link; as in [12], we use the color n to refer to the $(n+1)$–dimensional representation, so that the color $n=1$ corresponds to the usual Jones polynomial and Khovanov homology.) In this paper, we prove the following two extensions of [16].

Theorem 1.1 *There exists a colored Khovanov spectrum for any $\mathfrak{sl}_2(\mathbb{C})$ colored link. Its reduced cohomology is isomorphic to the colored Khovanov homology defined in Cooper and Krushkal* [2] *and Rozansky* [13].

Published: 9 April 2018 DOI: 10.2140/agt.2018.18.1411

Remark 1.2 In particular, the coloring $n=1$ (the 2–dimensional irreducible representation of $\mathfrak{sl}_2(\mathbb{C})$) assigned to each component of L produces a colored Khovanov spectrum agreeing with the construction of [7]. This fact already guarantees that there are links with colored spectra that are not wedge sums of Moore spaces; see Lipshitz and Sarkar [9]. In addition, the results of [16] imply that the 3–colored unknot also gives rise to non-Moore spaces.

Theorem 1.3 *There exists a Khovanov spectrum for any $\mathfrak{sl}_2(\mathbb{C})$ quantum spin network. Its reduced cohomology is isomorphic to the homology of the categorified spin networks defined in* [2].

Both the colored Khovanov homology and the categorified quantum spin networks mentioned in these theorems are defined using the categorified Jones–Wenzl projectors. Thus Theorems 1.1 and 1.3 will be viewed as special cases of a slightly more general theorem that can be stated as follows.

Theorem 1.4 *For any link diagram D involving a finite number of Jones–Wenzl projectors, there exists a Khovanov spectrum $\mathcal{X}(D)$ with reduced cohomology isomorphic to the homology defined using the categorified Jones–Wenzl projectors as in* [12] and [2].

An example of the type of diagram in the statement of Theorem 1.4 is provided in Figure 1. Notice that the Jones–Wenzl projectors themselves, and their categorifications, are defined using tangles. The Khovanov spectrum has not yet been defined for tangles, and so Theorem 1.4 requires that the projectors involved are closed in some way to form a link diagram. Nevertheless we will also prove several properties of such spectra, such as being "killed by turnbacks", that the projectors and their categorifications satisfy.

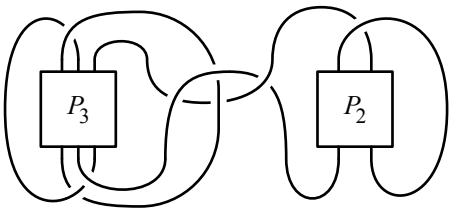

Figure 1: An example diagram for which Theorem 1.4 defines a Khovanov spectrum

The proof of Theorem 1.4 is a generalization of the proof in [16] for the torus links. With [12] in mind, we replace the projectors with torus braids, seeking a stabilization

of the spectra as the number of twists in each such braid goes to infinity. The strategy is similar to that in [16], but requires some new bounds and estimates that account for the presence of crossings away from the twisting, as well as the (possibly changing) orientations of the strands being twisted.

Remark 1.5 Theorem 1.1 was proved independently by Andrew Lobb, Patrick Orson, and Dirk Schuetz in [10], which appeared on the arXiv while this manuscript was in preparation. The authors further remark in that paper that their methods could be used to prove a statement similar to Theorem 1.4.

Remark 1.6 The Khovanov spectra of Theorem 1.4 will be constructed as homotopy colimits of the Khovanov spectra for link diagrams as defined in [7]. Up to a finite formal desuspension, the spectra of [7] are suspension spectra of CW complexes, and thus their homotopy colimits are also suspension spectra of CW complexes (the "suspension spectrum" functor from spaces to spectra preserves all homotopy colimits). Although these colimiting CW complexes are infinite, the stabilization mentioned above will mean that the resulting spectra will be stably homotopy equivalent to some finite term in the sequence.

With a well-defined colored Khovanov spectrum in hand, we follow the strategy of Rozansky in [13] to prove:

Theorem 1.7 *The Khovanov spectra of n–colored B–adequate links stabilize as $n \to \infty$.*

For a more detailed statement and an illustration of the stabilization, see Theorem 5.5 and Tables 1 and 2 in Section 5. Theorem 1.7 gives us the stable tail behavior for the Khovanov spectra of colored B–adequate links, matching the behavior of the colored homology and colored Jones polynomials. This theorem is a lifting of Theorem 2.2 in [13] to the stable homotopy category. The proof will be based on two main ideas. First we verify that all of the isomorphisms constructed in [13] between colored Khovanov homology groups lift to maps between the corresponding spectra. Second we ensure that the homological range of isomorphism for these maps (which depends on n) can be translated into a range of q–degrees for which all nonzero homology is isomorphic via these same maps. This will allow Whitehead's theorem to guarantee that the maps are stable homotopy equivalences.

Finally, we will also provide a more direct argument for the tail of the Khovanov spectrum of the colored unknot; that is, for $\mathcal{X}(T(n,\infty))$ as $n \to \infty$.

Theorem 1.8 *In the case of the unknot, the n–colored Khovanov spectra $\mathcal{X}(T(n,\infty))$ defined in* [16] *stabilize as $n \to \infty$, and the stable limit*

$$\mathcal{X}(T(\infty,\infty)) := \bigvee_{j\in(2\mathbb{N}\cup 0)} \mathcal{X}^j(T(\infty,\infty))$$

satisfies

$$\mathcal{X}^j(T(\infty,\infty)) \simeq \begin{cases} \mathcal{X}^0(T(j,\infty)) \simeq \mathcal{X}^{(j-1)^2}(T(j,j-1)) & \text{for } j>0,\\ \mathcal{X}^{-1}(T(1,\infty)) \simeq S^0 & \text{for } j=0,\end{cases}$$

where S^0 denotes the standard sphere spectrum.

For a more detailed visual representation of the statement of Theorem 1.8, see Table 3 in Section 6. The proof of Theorem 1.8 will use much simpler stable homotopy equivalences than the maps used to prove Theorem 1.7, and will also provide a sharper bound on the coloring n needed for stabilization in a given q–degree.

This paper is arranged as follows. In Section 2 we review the necessary background on Khovanov homology, the Khovanov spectrum, and the categorified Jones–Wenzl projectors as constructed in [12]. We also set our grading conventions for Khovanov homology used throughout the paper. In Section 3 we build the Khovanov spectrum for arbitrary diagrams involving Jones–Wenzl projectors, proving Theorem 1.4, and then derive some simple properties for these spectra similar to those satisfied by the projectors themselves. Section 4 contains a short description of quantum spin networks and colored links, allowing quick proofs of Theorems 1.1 and 1.3 via Theorem 1.4. Section 5 is devoted to proving Theorem 1.7. Finally, Section 6 contains the proof of Theorem 1.8, with one proof from this section placed in the appendix.

Acknowledgements The author would like to thank: the referee of this paper for several very helpful comments and suggestions; the referee of his prior paper [16] for bringing up the question of allowing $n \to \infty$ as in Theorem 1.8; Matt Hogancamp for calling attention to the properties of linking a 1–colored unknot with a colored link; and his advisor Slava Krushkal for his continued support and advice while preparing this paper. This research was supported in part by NSF grant DMS-1612159.

2 Background

2.1 Our grading conventions for Khovanov homology

For the original definition of the Khovanov homology of a link, see [5]. We quickly summarize here the main points. Any crossing $\times$ in a link diagram can be resolved

in one of two ways: with a 0–resolution $\rangle\langle$ or with a 1–resolution $\asymp$. The Khovanov chain complex $\mathrm{KC}^{i,j}(L)$ of a link diagram L is a bigraded chain complex built out of a cube of resolutions of the diagram L. The generators of $\mathrm{KC}^{i,j}(L)$ correspond to assignments of v_+ or v_- to each circle in any given resolution. There are several different conventions in the literature for the precise meaning of the two gradings i and j. In this paper, following [7] and [1], we shall let i refer to the homological grading and j refer to the q–grading, which we define by

$$\deg_h(\cdot) := \#(\text{1–resolutions}) - n^-, \tag{1}$$

$$\deg_q(\cdot) := \#(\text{1–resolutions}) + (\#(v_+) - \#(v_-)) + (n^+ - 2n^-), \tag{2}$$

where n^+ and n^- denote the number of positive and negative crossings respectively in the diagram for L. Under these grading conventions, the Khovanov differential increases $\deg_h$ by one and respects $\deg_q$, allowing $\mathrm{KC}^{i,j}(L)$ to split as a direct sum over q–degree. The resulting homology groups are then bigraded invariants of the link, with no shifts necessary for any Reidemeister moves on the diagram used. In what follows, the q–grading normalization shift $n^+ - 2n^-$ will often be denoted by N.

2.2 The Khovanov homotopy type

Given a link L in S^3, we shall let $\mathcal{X}(L) = \bigvee_{j\in\mathbb{Z}} \mathcal{X}^j(L)$ denote the Khovanov spectrum of the link L. For the full description of this invariant, see [7]. We summarize the important points about $\mathcal{X}(L)$ here:

- $\mathcal{X}(L)$ is the suspension spectrum of a CW complex.
- $\widetilde{H}^i(\mathcal{X}^j(L)) = \mathrm{Kh}^{i,j}(L)$, the Khovanov homology of the link L (see Equations (1) and (2) for our grading conventions).
- Each $\mathcal{X}^j(L)$ is constructed combinatorially using the Khovanov chain complex $\mathrm{KC}^j(L)$ in q–degree j, together with a choice of "ladybug matching" that uses the diagram for L (see Section 5.4 in [7]). Note that since $\mathrm{KC}^j(L)$ is nontrivial for only finitely many q–degrees j, the wedge sum above is actually finite.
- Each $\mathcal{X}^j(L)$ is an invariant of the link L. That is to say, the stable homotopy type of $\mathcal{X}^j(L)$ does not depend on the diagram used to portray L, nor on the various choices that are made during the construction.
- Nontrivial Steenrod square operations on $\widetilde{H}^i(\mathcal{X}^j(L);\mathbb{Z}/2\mathbb{Z}) = \mathrm{Kh}^{i,j}(L;\mathbb{Z}/2\mathbb{Z})$ can serve to differentiate links with isomorphic Khovanov homology [9] and also give

rise to slice genus bounds [8]. One corollary of the work in [16] gives the existence of nontrivial Sq^2 for infinitely many 3–strand torus links. See further calculations in [10]. gbr The most important property of $\mathcal{X}(L)$ for our purposes comes from the following "collapsing lemma", a slight generalization of that appearing in Section 2.2 of [16]. Fixing $j \in \mathbb{Z}$, we consider the Khovanov chain complex $\mathrm{KC}(L)$ represented as the mapping cone of a chain map

$$\mathrm{KC}^{j+N_L}(L) = (\mathrm{KC}^{j+N_{L''}}(L'') \to \mathrm{KC}^{j-1+N_{L'}}(L')), \tag{3}$$

where L' and L'' are the links resulting from taking the 1–resolution and 0–resolution, respectively, of a single crossing in the diagram for L. The superscripts stand for q–gradings, with N_L denoting the q–degree normalization shift $n^+ - 2n^-$ in the link diagram L, and similarly for $N_{L'}$ and $N_{L''}$. There is a corresponding cofibration sequence of spectra (see Theorem 2 in [7])

$$\Sigma^a \mathcal{X}^{j+N_{L''}}(L'') \hookrightarrow \mathcal{X}^{j+N_L}(L) \twoheadrightarrow \Sigma^b \mathcal{X}^{j-1+N_{L'}}(L'), \tag{4}$$

where the Σ stands for suspensions allowing for shifts in homological degree, with $a = n^-_{L''} - n^-_L$ and $b = n^-_{L'} - n^-_L + 1$, the differences in the count of negative crossings n^- for the various diagrams (the extra $+1$ for L' takes into account the loss of a 1–resolution from the point of view of L'). See Equations (1) and (2) above to clarify the grading shifts.

Lemma 2.1 *With* $\mathrm{KC}^{j+N_L}(L) = \big(\mathrm{KC}^{j+N_{L''}}(L'') \to \mathrm{KC}^{j-1+N_{L'}}(L')\big)$ *as above, we have:*

- *If* $\mathrm{KC}^{j-1+N_{L'}}(L')$ *is acyclic, then the induced inclusion*

$$\Sigma^a \mathcal{X}^{j+N_{L''}}(L'') \hookrightarrow \mathcal{X}^{j+N_L}(L)$$

  is a stable homotopy equivalence.

- *If* $\mathrm{KC}^{j+N_{L''}}(L'')$ *is acyclic, then the induced surjection*

$$\mathcal{X}^{j+N_L}(L) \twoheadrightarrow \Sigma^b \mathcal{X}^{j-1+N_{L'}}(L')$$

  is a stable homotopy equivalence.

Proof See the brief sketch in [16], which describes the first case for positive crossings. Both cases are special cases of Lemma 3.32 in [7], presented as in Theorem 2 from the same paper. □

Lemma 2.1 says that we can resolve crossings in a diagram one at a time, and if one resolution of a crossing results in a diagram with an acyclic chain complex in the specified q–degree, this entire part of the full chain complex can be collapsed and we are left with the chain complex using only the other resolution (up to some potential suspensions). Just as in [16], we will want to make repeated use of this idea here.

2.3 A categorified Jones–Wenzl projector

The n^{th} *Jones–Wenzl projector* P_n is a special idempotent element in the Temperley–Lieb algebra TL_n on n strands over coefficient field $\mathbb{C}(q)$, which is characterized by the following axioms:

I. $P_n \cdot e_i = e_i \cdot P_n = 0$ for any of the standard multiplicative generators $e_i =$  in TL_n. This is often described by stating that P_n is "killed by turnbacks".

II. The coefficient of the n–strand identity tangle in the expression for P_n is 1.

(For the original definition of the P_n, see [15]; for an account of the Temperley–Lieb algebra, the P_n, and some of their uses in 3–manifold theory, see [4].)

In [12] Lev Rozansky provided a categorification for any P_n via an infinite torus braid. If we let $\sigma_1, \dots, \sigma_{n-1}$ denote the standard generators of the braid group B_n, we introduce the following notation for full twists on n strands:

$$\boldsymbol{T}_n^k := (\sigma_1 \sigma_2 \cdots \sigma_{n-1})^{nk}. \tag{5}$$

After giving a well-defined notion for a stable limit of chain complexes, Rozansky proved the following theorem.

Theorem 2.2 *The Khovanov chain complexes associated to the braids* $\mathrm{KC}(\boldsymbol{T}_n^k)$ *stabilize up to chain homotopy as* $k \to \pm\infty$. *The limiting complex* $\mathrm{KC}(\boldsymbol{T}_n^{\pm\infty})$ *satisfies the following properties:*

I. *Adding a turnback onto the top or bottom of* $\mathrm{KC}(\boldsymbol{T}_n^{\pm\infty})$ *causes the entire complex to be chain homotopic to a trivial complex.*

II. *The resulting complex can be viewed as a mapping cone of a map from (for* $+\infty$*) or to (for* $-\infty$*) the* 1*–term complex of the identity tangle, where the other terms involve only nonidentity tangles in nonzero homological degrees.*

Proof See [12], and also Section 1.6 in [13]. □

This theorem means that, to obtain a chain complex categorifying the Jones–Wenzl projectors up through a given homological degree, it is enough to replace any P_n in a diagram with a copy of $\boldsymbol{T}_n^{\pm k}$ for large k (we shall often refer to this as a "finite-twist approximation"). The exact size of k needed depends on the homological degree we are interested in. The graded Euler characteristic of this complex stabilizes as $k \to \infty$ to give a power series representation of the rational terms appearing in the usual formulas for the P_n. Positive (right-handed) twisting gives a power series in q, while negative (left-handed) twisting gives a power series in q^{-1}.

Remark 2.3 At around the same time, Ben Cooper and Slava Krushkal independently constructed a categorification of the Jones–Wenzl projectors in [2]. We are unsure if it is possible to lift their construction to the Khovanov spectrum in general; see [10] for some further remarks and a lifting in the $n = 2$ case. Also, in [6], Mikhail Khovanov introduced separate categorifications for the colored Jones polynomial using renormalizations to eliminate the denominators present in the terms of the Jones–Wenzl projectors. Our approach here aims to recover Rozansky's version outlined above rather than these alternative categorifications (although the categorified projectors in [2] are chain homotopic to those produced in [12]; see Section 3 of [2]).

The first goal of this paper is to properly lift Theorem 2.2 to a similar statement about Khovanov spectra. However, Theorem 2.2 is a statement about complexes of tangles. As mentioned in the introduction, the Khovanov spectrum has not yet been defined for tangles in general, and only exists for links. This is the reason for the slightly indirect phrasing of Theorem 1.4, which can be viewed as a statement about having Khovanov spectra for Jones–Wenzl projectors that are closed up in any fashion in S^3. We turn now to the proof of Theorem 1.4.

3 A Khovanov spectrum for diagrams involving Jones–Wenzl projectors

3.1 Basic notation and a key counting lemma

We begin with some general notation for use throughout this section.

- $n \in \mathbb{N}$ will always denote a number of strands for various purposes (typically for a given torus braid or, later, for an n–strand cabling of a link diagram).
- Boldface capital letters will refer to braids and/or tangles within a diagram.

- $\boldsymbol{I_n}$ will denote the identity braid on n strands.
- $\boldsymbol{T_n^k}$ will denote a torus braid on n strands with k full right-handed (positive) twists (see Equation (5)).
- $\boldsymbol{T_n^{-k}}$ will denote such a torus braid with k full left-handed (negative) twists.
- $\boldsymbol{Z}$ will often be used to denote an arbitrary tangle.
- We will use the inner-product notation $\langle \boldsymbol{Z}_1, \boldsymbol{Z}_2 \rangle$ to indicate connecting two tangles top to top and bottom to bottom. This notation is meant to imitate the inner product in the Temperley–Lieb algebra. See Figure 2.
- $\boldsymbol{Z}^{\cap i}$ will be used to indicate that the i^{th} and $(i+1)^{\text{st}}$ strands at the top of the tangle $\boldsymbol{Z}$ are being capped off. Similarly, $\boldsymbol{Z}_{\cup i}$ will indicate capping off the i and $i+1$ strands at the bottom. See Figure 2.

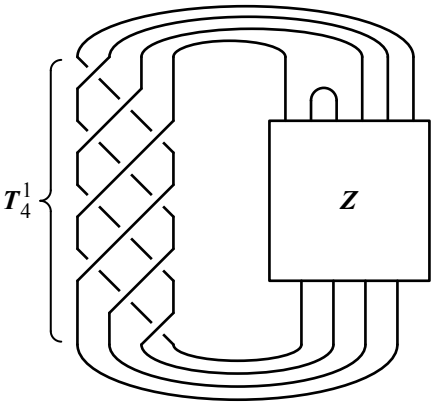

Figure 2: The diagram $\langle \boldsymbol{T}_4^1, \boldsymbol{Z}^{\cap 2} \rangle$. $\boldsymbol{T}_4^1$ indicates the full right-handed twist on 4 strands, and $\boldsymbol{Z}$ is some fixed $(6,4)$–tangle. The $\cap 2$ indicates a cap on the 2^{nd} and 3^{rd} strands above $\boldsymbol{Z}$.

In many link diagrams in this paper, a single copy of $\boldsymbol{T_n^{\pm k}}$ will be singled out for consideration, allowing the diagram to be viewed as $\langle \boldsymbol{T_n^{\pm k}}, \boldsymbol{Z} \rangle$ for some tangle $\boldsymbol{Z}$ (similar to Figure 2, but without the cap). In these situations, we will also view the normalization shifts of Equations (1) and (2) as split into contributions based on the $\boldsymbol{T_n}$ and the $\boldsymbol{Z}$ as in the following definition.

Definition 3.1 In a link diagram L viewed as $L = \langle \boldsymbol{T_n^{\pm k}}, \boldsymbol{Z} \rangle$ as above, the symbol τ will be used to denote the q–normalization shift $n^+ - 2n^-$ counting only crossings within *one full twist* of the n strands (that is, within $\boldsymbol{T_n^{\pm 1}}$). Similarly, the symbol η

will be used to denote the homological normalization shift n^- counting only crossings within *one full twist*. The symbol $N_{\boldsymbol{Z}}$ will be used to denote the q–normalization shift n^+-2n^- counting only crossings within the tangle $\boldsymbol{Z}$. More generally, N_D will denote the shift n^+-2n^- counting crossings within a diagram D (whether tangle or otherwise).

We will have no need for the homological normalization shift n^- counting only crossings in $\boldsymbol{Z}$.

Remark 3.2 Notice that these shifts τ, η and $N_{\boldsymbol{Z}}$ depend on the orientation of the strands, and allowable orientations are affected by the *full link diagram involved*, not just the piece being counted. In Figure 2 for example, the value of τ depends heavily on the tangle $\boldsymbol{Z}$, despite the fact that it only counts crossings within the $\boldsymbol{T}_4^1$. In cases where the tangle $\boldsymbol{Z}$ is changing, subscripts will be attached to the symbol τ as necessary to indicate which full diagram is being considered. Similarly, if there are multiple $\boldsymbol{T}_{n_i}$ to consider within some single link diagram, the subscript i will be used for the shifts τ_i and η_i to indicate which twist is being considered.

In order to illustrate these notations, we prove the following very simple observation about full twists that indicates why they are preferable to work with (as opposed to the fractional twists that were sufficient in [16]).

Lemma 3.3 *For any (n,n)–tangle $\boldsymbol{Z}$, consider the diagram $D(k) := \langle \boldsymbol{T}_n^k, \boldsymbol{Z} \rangle$. Then all of the $D(k)$ are links with the same number of strands, which can be oriented equivalently for all k. Thus $N_{D(k)} = k\tau + N_{\boldsymbol{Z}}$ with $N_{\boldsymbol{Z}}$ and τ independent of k; in particular, $N_{\boldsymbol{Z}}$ can be determined by the diagram $D(0) = \langle \boldsymbol{I}, \boldsymbol{Z} \rangle$. Similarly, for such a diagram, η is also independent of k.*

Proof In a full twist, any strand takes the i^{th} point at the top to the i^{th} point on the bottom, so for the purposes of counting and orienting the strands, this is equivalent to the identity braid $\boldsymbol{I}$. The orientations of the strands are all that matters for calculating $N_{\boldsymbol{Z}}$, and also for calculating τ and η. Since τ counts positive and negative crossings for one full twist, k full twists will contribute $k\tau$. □

Remark 3.4 The previous observation was written and notated for positive full twists, but it is clear that the exact same argument holds for negative full twists as well. This will be typical of several of the arguments later in this section.

We conclude this section with the key counting lemma which is used essentially throughout the paper. This lemma can be viewed as a generalization of Lemma 3.5 in [16], which itself was just a restatement of Marko Stošić's Lemma 1 in [14].

Lemma 3.5 *Fix $n \geq 2$ in $\mathbb{N}$. For any $i \in \{1, 2, \dots, n-1\}$ and any $(n-2, n)$–tangle $\boldsymbol{Z}$, consider the link diagram $D_\pm = \langle (\boldsymbol{T}_n^{\pm k})^{\cap i}, \boldsymbol{Z} \rangle$. That is, consider any closure of $\boldsymbol{T}_n^{\pm k}$ involving at least one turnback at the top. Then for any chosen orientation of the strands, we have:*

- *This link diagram is isotopic to $D'_\pm = \langle \boldsymbol{T}_{n-2}^{\pm k}, \boldsymbol{Z}_{\cup n-i} \rangle$.*
- *Letting $\tau_\pm$ count $n^+ - 2n^-$ for crossings from $\boldsymbol{T}_n$ in $D_\pm$ and letting $\tau'_\pm$ count this shift for crossings from $\boldsymbol{T}_{n-2}$ in $D'_\pm$, we have*

$$\tau'_+ = \tau_+ + 2n, \tag{6}$$

$$\tau'_- = \tau_- + 2n - 6. \tag{7}$$

Proof We pull the turnback through the full twists, which corresponds to pulling out two "parallel" strands wrapping around the cylinder defining the torus braid. As in Lemma 3.3, using full twists ensures that the turnback "exits" the torus braid at the same two points that it entered, which swing around to give the $(n-i)^{\text{th}}$ and $(n-i+1)^{\text{st}}$ points at the bottom of $\boldsymbol{Z}$. This leaves us with $n-2$ strands for the torus braid, still with the same amount of twisting. See Figure 3. This proves the first point.

To prove the second point, we first note that the total number of crossings in a full twist on n strands is $n(n-1)$, while the total number for a full twist on $n-2$ strands is $(n-2)(n-3)$. This means that when pulling the turnback through, we managed to eliminate $4n-6$ crossings. One full twist of these two strands corresponds to two Reidemeister I moves; the other $4n-8$ eliminations all must have come from Reidemeister II moves. Regardless of the type of twist and the orientation of the strands, all of these Reidemeister II moves would have eliminated one positive and one negative crossing each. The two Reidemeister I moves would have eliminated negative crossings from a positive twist, or eliminated positive crossings from a negative twist. Again, this is independent of the orientation of the strands. Calculating the effect of these eliminations on the normalization $n^+ - 2n^-$ gives the result. □

Remark 3.6 There is no difference in having the turnback at the bottom of the $\boldsymbol{T}_n^{\pm k}$. The proof makes it clear that it ends up at the top of the $\boldsymbol{Z}$ in that case.

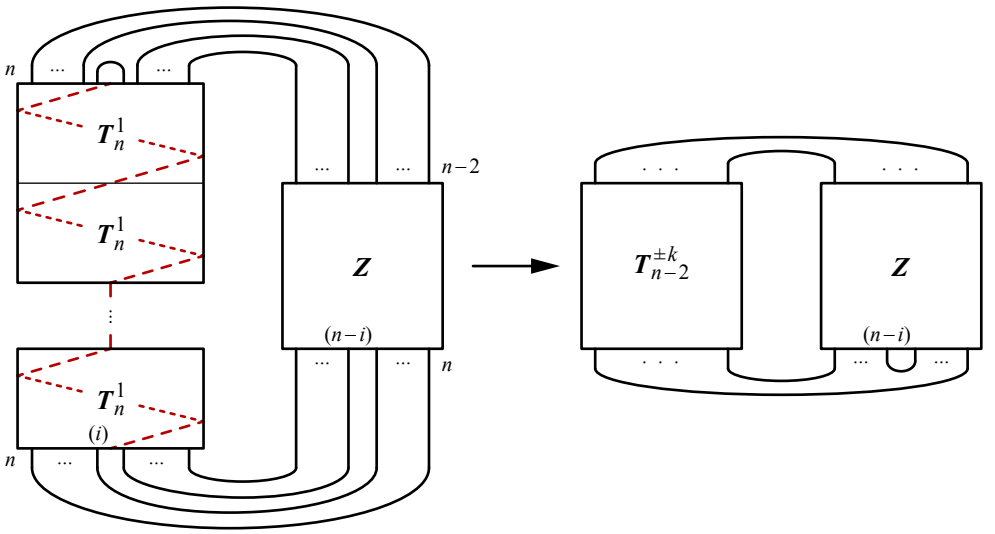

Figure 3: The diagram $\langle (T_n^{\pm k})^{\cap i}, Z \rangle$ with the $T_n^{\pm k}$ drawn as separate copies of T_n^1. The cap is pulled through the twists as shown (the dashed red line would be for $+k$; the opposite direction would be taken for $-k$). The n and $n-2$ show the number of strands entering and exiting at various points. The (i) at the bottom of the twisting indicates the i^{th} strand counted from the left, and similarly for the $(n-i)$ at the bottom of Z.

3.2 Proving Theorem 1.4

Let D denote a link diagram involving a finite number of Jones–Wenzl projectors. More precisely, D is obtained from a link diagram by formally replacing a finite number of identity braids I_{n_i} with Jones–Wenzl projectors P_{n_i} (see Figure 1 in the introduction provides clarification). Just as in Section 7 of [16], we would like to define $\mathcal{X}^j(D)$ as the homotopy colimit of a sequence of spectra of finite link diagrams that stabilizes as the twisting in the diagram goes to infinity. To do this we focus on a single projector at a time. Towards that end, we combine Lemmas 2.1 and 3.3 to establish the following two sequences.

Proposition 3.7 *Fix $n \in \mathbb{N}$ and $j \in \mathbb{Z}$. Let Z be an arbitrary (n,n)–tangle. Then the maps of Lemma 2.1 provide the following two sequences (one for right-handed twists, one for left-handed twists):*

$$\begin{aligned}(8)\qquad \mathcal{X}^{j+N_Z}(\langle T_n^0, Z\rangle) \hookrightarrow \Sigma^{\eta}\mathcal{X}^{j+N_Z+\tau}(\langle T_n^1, Z\rangle) \hookrightarrow \cdots \\ \hookrightarrow \Sigma^{k\eta}\mathcal{X}^{j+N_Z+k\tau}(\langle T_n^k, Z\rangle) \hookrightarrow \cdots,\end{aligned}$$

$$(9)\qquad \mathcal{X}^{j+N_{\boldsymbol{Z}}}(\langle \boldsymbol{T}_n^0, \boldsymbol{Z}\rangle) \twoheadleftarrow \cdots \twoheadleftarrow \Sigma^{k(\eta-n(n-1))}\mathcal{X}^{j+N_{\boldsymbol{Z}}+k\tau+kn(n-1)}(\langle \boldsymbol{T}_n^{-k}, \boldsymbol{Z}\rangle) \twoheadleftarrow \cdots,$$

where the symbols η, τ, and $N_{\boldsymbol{Z}}$ are as defined in Definition 3.1.

Proof To build the right-handed sequence (8), we "start" with the $(k+1)^{\text{st}}$ term and resolve crossings within one of the full twists one at a time until we reach the k^{th} term. Specifically, we consider the diagram $\langle \boldsymbol{T}_n^{k+1}, \boldsymbol{Z}\rangle = \langle \boldsymbol{T}_n^k, \boldsymbol{T}_n^1 \cdot \boldsymbol{Z}\rangle$, where we use the product notation to indicate concatenation (see Figure 4). We number the crossings of the $\boldsymbol{T}_n^1$ sitting above $\boldsymbol{Z}$ starting from the "topmost" such crossing. Then each inclusion in (8) will be defined as the composition of $n(n-1)$ inclusions coming from (4) by resolving these numbered crossings as 0–resolutions in this order (note that the all-zero resolution of $\boldsymbol{T}_n^1$ is precisely $\boldsymbol{I}_n$).

We now introduce some notation similar to the notation in Section 3 of [16]. Let $\boldsymbol{D}_0 := \boldsymbol{T}_n^1 \cdot \boldsymbol{Z}$. Then for each $i = 1, 2, \ldots, n(n-1)$, let $\boldsymbol{D}_i$ denote the diagram obtained from $\boldsymbol{D}_{i-1}$ by resolving the i^{th} crossing with a 0–resolution, and let $\boldsymbol{E}_i$ denote the diagram obtained from $\boldsymbol{D}_{i-1}$ (*not* from $\boldsymbol{E}_{i-1}$; this will change for the left-handed sequence) by resolving the i^{th} crossing with a 1–resolution. Thus $\boldsymbol{D}_i$ will have all crossings up to the i^{th} resolved as 0–resolutions, while $\boldsymbol{E}_i$ will have all crossings up to the $(i-1)^{\text{st}}$ resolved as 0–resolutions, but the i^{th} as a 1–resolution. This arrangement allows us to see, at each step i, the cofibration sequence (ignoring the homological shifts)

$$(10)\qquad \mathcal{X}^{j+N_{\boldsymbol{D}_i}+k\tau_{\boldsymbol{D}_i}}(\langle \boldsymbol{T}_n^k, \boldsymbol{D}_i\rangle) \hookrightarrow \mathcal{X}^{j+N_{\boldsymbol{D}_{i-1}}+k\tau_{\boldsymbol{D}_{i-1}}}(\langle \boldsymbol{T}_n^k, \boldsymbol{D}_{i-1}\rangle) \twoheadrightarrow \mathcal{X}^{j+N_{\boldsymbol{E}_i}+k\tau_{\boldsymbol{E}_i}-1}(\langle \boldsymbol{T}_n^k, \boldsymbol{E}_i\rangle).$$

For further clarification, see Figure 4. Notice the subscripts on the τ terms: the orientations (and thus positive/negative crossing information) of the strands within $\boldsymbol{T}_n^k$ may change when resolving crossings (see Remark 3.2). However, we also know from Lemma 3.3 that all of the τ_* terms and N_* terms are *independent of* k. The final term $\boldsymbol{D}_{n(n-1)}$ is precisely $\boldsymbol{Z}$, so Lemma 3.3 allows the τ and $N_{\boldsymbol{Z}}$ terms to be preserved as indicated in the sequence (8). The suspensions giving the homological shifts are clear: we are counting the number of negative crossings introduced in a new twist.

The left-handed sequence (9) is built using compositions of the surjections of the cofibration sequence (4), since the left-handed twist $\boldsymbol{T}_n^{-1}$ needs an all-one resolution to give the identity braid $\boldsymbol{I}_n$. For this reason, the roles of the $\boldsymbol{D}_i$ and $\boldsymbol{E}_i$ are swapped, and

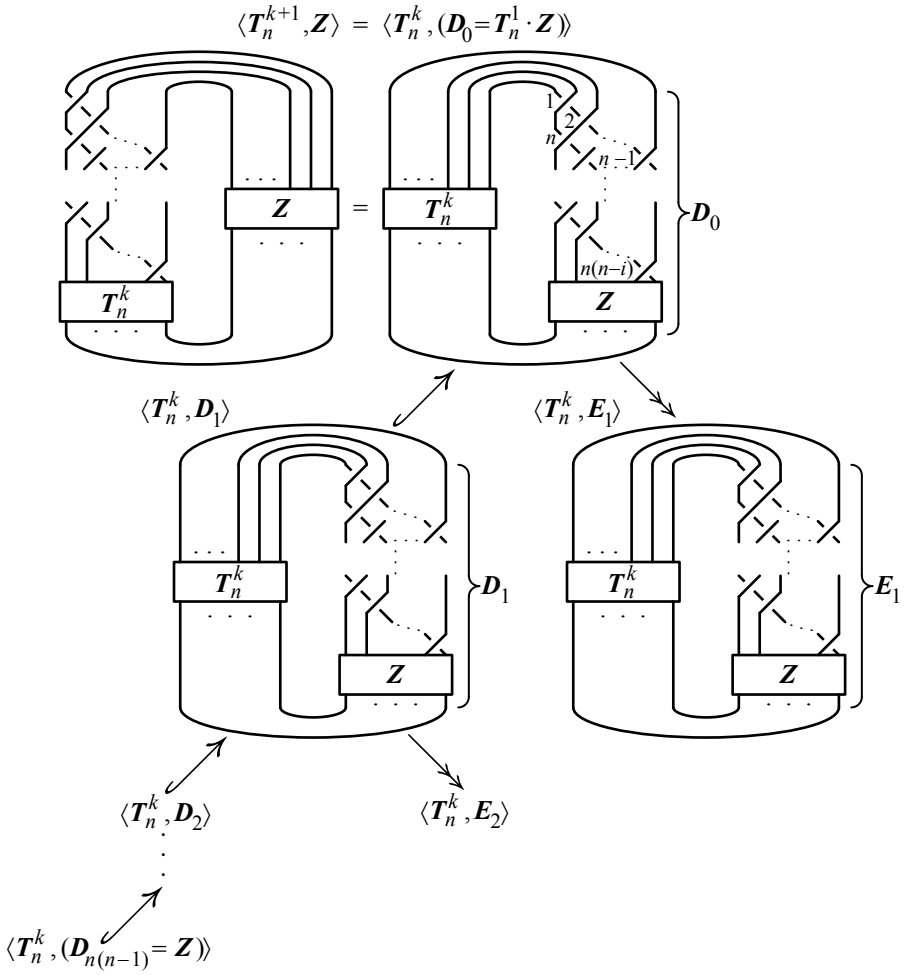

Figure 4: Building a single map in the sequence (8) as a composition of inclusions coming from resolving crossings as in Lemma 2.1. The numbering on the crossings in the diagram $\langle \boldsymbol{T}_n^k, \boldsymbol{D}_0 \rangle$ indicates the order in which we resolve crossings. $\boldsymbol{D}_1$ and $\boldsymbol{E}_1$ are illustrated as well, with the first crossing resolved. Note that $\boldsymbol{E}_2$ is obtained from $\boldsymbol{D}_1$, not from $\boldsymbol{E}_1$. Thus any $\boldsymbol{E}_i$ will have precisely one cup/cap.

their definitions change slightly. To prevent confusion, we use new names $\boldsymbol{F}_i$ and $\boldsymbol{G}_i$ and define $\boldsymbol{G}_0 := \boldsymbol{T}_n^{-1} \cdot \boldsymbol{Z}$, and let $\boldsymbol{G}_i$ denote the diagram obtained from $\boldsymbol{G}_{i-1}$ by resolving the i^{th} crossing with a 1–resolution, and let $\boldsymbol{F}_i$ denote the diagram obtained from $\boldsymbol{G}_{i-1}$ by resolving the i^{th} crossing with a 0–resolution. Pictorially the $\boldsymbol{G}_i$ match the $\boldsymbol{D}_i$ from above, and the $\boldsymbol{F}_i$ match the $\boldsymbol{E}_i$, but in the cofibration sequences we see,

again ignoring homological shifts,

$$\begin{aligned}(11)\quad \mathcal{X}^{j+(k+1)n(n-1)-(i-1)+N_{\boldsymbol{F}_i}+k\tau_{\boldsymbol{F}_i}}(\langle \boldsymbol{T}_n^{-k}, \boldsymbol{F}_i\rangle)&\\ \hookrightarrow \mathcal{X}^{j+(k+1)n(n-1)-(i-1)+N_{\boldsymbol{G}_{i-1}}+k\tau_{\boldsymbol{G}_{i-1}}}(\langle \boldsymbol{T}_n^{-k}, \boldsymbol{G}_{i-1}\rangle)&\\ \twoheadrightarrow \mathcal{X}^{j+(k+1)n(n-1)-i+N_{\boldsymbol{G}_i}+k\tau_{\boldsymbol{G}_i}}(\langle \boldsymbol{T}_n^{-k}, \boldsymbol{G}_i\rangle).&\end{aligned}$$

Notice the extra shifts of $i-1$ and i, which occur because we have been "losing" 1–resolutions along the way. We can see that, once $i=n(n-1)$, we arrive at $j+kn(n-1)$ together with the normalization terms, as desired for $\langle \boldsymbol{T}_n^{-k}, \boldsymbol{Z}\rangle$ in sequence (9). We use Lemma 3.3 in the same way to guarantee that the $N_{\boldsymbol{Z}}$ and τ terms don't change, and we also see the extra homological shift due to losing 1–resolutions as we go. □

Proposition 3.8 *Fix $j\in\mathbb{Z}$ and $n\geq 2$ in $\mathbb{N}$. Then for any (n,n)–tangle $\boldsymbol{Z}$, both sequences* (8) *and* (9) *stabilize. That is, there exist bounds b^+ and b^- such that the maps in* (8) *are all stable homotopy equivalences for $k\geq b^+$, and similarly for $k\geq b^-$ for the maps in* (9)*. Furthermore, b^+ depends only on j and the all-zero resolution of $\boldsymbol{Z}$, while b^- depends on j, the number of crossings in $\boldsymbol{Z}$, and the all-one resolution of $\boldsymbol{Z}$.*

Proof We will prove the stabilization of the two sequences separately to highlight the slight differences between the two. The notations $\boldsymbol{D}_i$, $\boldsymbol{E}_i$, $\boldsymbol{F}_i$ and $\boldsymbol{G}_i$ introduced in the previous proof will be used throughout. Both cases will be similar to the arguments in [16].

Focusing first on the right-handed case, we consider the cofibration sequences (10). By Lemma 2.1, as long as all the Khovanov chain complexes $\mathrm{KC}^{j+N_{\boldsymbol{E}_i}+k\tau_{\boldsymbol{E}_i}-1}(\langle \boldsymbol{T}_n^k, \boldsymbol{E}_i\rangle)$ are acyclic, the inclusions in Equation (10) will be stable homotopy equivalences for all $i=1,\dots,n(n-1)$, allowing us to conclude that their composition (which is the map in the sequence (8)) is as well. Let $\min_q(\cdot)$ be the minimal q–degree of nonzero Khovanov homology for a link diagram. Our goal now is to find a bound b^+ so that, for all $i=1,\dots,n(n-1)$,

$$(12)\qquad j+N_{\boldsymbol{E}_i}+k\tau_{\boldsymbol{E}_i}-1<\min_q(\langle \boldsymbol{T}_n^k, \boldsymbol{E}_i\rangle)\quad \text{for all } k\geq b^+.$$

Figure 5 illustrates the key point of the proof. The diagram $\langle \boldsymbol{T}_n^k, \boldsymbol{E}_i\rangle$ has a turnback at the "top" of E_i that can be swung around and "pulled through" the twisting $\boldsymbol{T}_n^k$ and then back around to the bottom of E_i, just as in Lemma 3.5. Let E_i' denote the resulting tangle, so that we have $\langle \boldsymbol{T}_n^k, \boldsymbol{E}_i\rangle$ isotopic to $\langle \boldsymbol{T}_{n-2}^k, \boldsymbol{E}_i'\rangle$. Since Khovanov

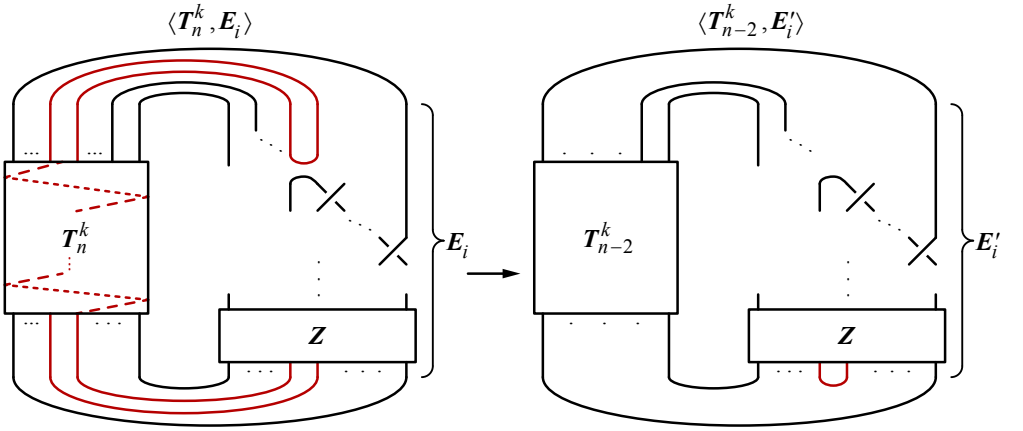

Figure 5: Pulling the turnback in $\langle T_n^k, E_i\rangle$ through the twists to get $\langle T_{n-2}^k, E_i'\rangle$. The turnback and its path are indicated in red. Note that none of the crossings in E_i (including Z) are affected.

homology is an isotopy invariant, we must have

$$\min_q(\langle T_n^k, E_i\rangle) = \min_q(\langle T_{n-2}^k, E_i'\rangle). \tag{13}$$

Now just as in the proof of Lemma 3.12 in [16], the minimal q–degree of nonzero Khovanov homology for a diagram is bounded below by the minimal possible q–degree in the entire Khovanov chain complex, which occurs in the all-zero resolution by decorating all of the circles with v_-. The all-zero resolution of the crossings coming from Ts give identity braids, and so we have

$$\min_q(\langle T_{n-2}^k, E_i'\rangle) \geq -\#\mathrm{circ}(\langle I_{n-2}, Z_{\cup\iota,\text{all-zero}}^{\cap\iota}\rangle) + k\tau'_{E_i'} + N_{E_i'}. \tag{14}$$

Here $\#\mathrm{circ}(\cdot)$ indicates the number of circles present in the planar diagram, while $\iota := i \bmod (n-1)$. The "all-zero" subscript indicates that all of the crossings in $Z_{\cup\iota}^{\cap\iota}$ have been resolved into zero-resolutions. The τ' term and the N term are the n^+-2n^- normalization terms as usual. The τ' indicates that we are counting positive and negative crossings from T_{n-2} as opposed to τ that was counting such crossings in T_n (see the notation used in Lemma 3.5).

Since we performed an isotopy to get from E_i to E_i', the orientations of the strands did not change. Furthermore, no crossings were added to or removed from E_i. Thus $N_{E_i} = N_{E_i'}$, and $\tau'_{E_i'}$ can be viewed as τ'_{E_i}. We then use (6) from Lemma 3.5 to deduce

$$\min_q(\langle T_{n-2}^k, E_i'\rangle) \geq -\#\mathrm{circ}(\langle I_{n-2}, Z_{\cup\iota,\text{all-zero}}^{\cap\iota}\rangle) + k(\tau_{E_i} + 2n) + N_{E_i}. \tag{15}$$

Combining (12), (13) and (15) gives us the following new goal for our bound b^+:

$$j + N_{\boldsymbol{E}_i} + k\tau_{\boldsymbol{E}_i} - 1 < -\#\operatorname{circ}(\langle \boldsymbol{I}_{n-2}, \boldsymbol{Z}^{\cap \iota}_{\cup \iota,\text{all-zero}}\rangle) + k(\tau_{\boldsymbol{E}_i} + 2n) + N_{\boldsymbol{E}_i} \tag{16}$$

for all $k \geq b^+$. This is clearly satisfied for all i by choosing

$$b^+ := \max_{\iota=1,\dots,n-1} \frac{j + \#\operatorname{circ}(\langle \boldsymbol{I}_{n-2}, \boldsymbol{Z}^{\cap \iota}_{\cup \iota,\text{all-zero}}\rangle)}{2n}. \tag{17}$$

We see clearly from the definition of b^+ that it depends only on j and the all-zero resolution of $\boldsymbol{Z}$, as claimed. The final homological shift is clear.

We now turn to the left-handed sequence (9). The strategy is very similar so we will be brief. This time we consider the cofibration sequence (11), where our goal is to bound k to ensure that all of the $\mathrm{KC}^{j-(i-1)+N_{\boldsymbol{F}_i}+k\tau_{\boldsymbol{F}_i}}(\langle \boldsymbol{T}_n^{-k}, \boldsymbol{F}_i\rangle)$ are acyclic, ensuring that the surjections give stable homotopy equivalences.

Since the $\boldsymbol{F}_i$ pictorially match the $\boldsymbol{E}_i$ from before, we can still use Lemma 3.5 in the same way to arrive at $\langle \boldsymbol{T}_{n-2}^{-k}, \boldsymbol{F}_i'\rangle$ with corresponding τ'. Now comes the main difference between the left- and right-handed sequences. For the right-handed twist, the all-zero resolution of $\boldsymbol{T}_{n-2}^{k}$ is just $\boldsymbol{I}_n$; in particular, it is independent of k. Taking 0–resolutions motivates bounding based on the minimal q–degree. But for the left-handed twist, it is the all-one resolution of $\boldsymbol{T}_n^{-k}$ that is just $\boldsymbol{I}_n$. Taking 1–resolutions motivates bounding based on the maximal q–degree. So we define $\max_q(\cdot)$ to be the maximal q–degree of nonzero Khovanov homology for a given diagram, which is bounded above by the maximal q–degree for the full Khovanov chain complex. Following the logic of the right-handed case, we get

$$\begin{aligned}
\max_q(\langle \boldsymbol{T}_n^{-k}, \boldsymbol{F}_i\rangle) &= \max_q(\langle \boldsymbol{T}_{n-2}^{-k}, \boldsymbol{F}_i'\rangle) \\
&\leq \#\operatorname{cros}(\langle \boldsymbol{T}_{n-2}^{-k}, \boldsymbol{F}_i'\rangle) + \#\operatorname{circ}(\langle \boldsymbol{I}_{n-2}, \boldsymbol{Z}^{\cap \iota}_{\cup \iota,\text{all-one}}\rangle) + k(\tau'_{\boldsymbol{F}_i'}) + N_{\boldsymbol{F}_i} \\
&= (k(n-2)(n-3) + (n(n-1)-i) + \#\operatorname{cros}(\boldsymbol{Z})) \\
&\qquad + \#\operatorname{circ}(\langle \boldsymbol{I}_{n-2}, \boldsymbol{Z}^{\cap \iota}_{\cup \iota,\text{all-one}}\rangle) + k(\tau_{\boldsymbol{F}_i} + 2n - 6) + N_{\boldsymbol{F}_i} \\
&= k(n^2 - 3n + \tau_{\boldsymbol{F}_i}) + (n(n-1)-i) + \#\operatorname{cros}(\boldsymbol{Z}) \\
&\qquad + \#\operatorname{circ}(\langle \boldsymbol{I}_{n-2}, \boldsymbol{Z}^{\cap \iota}_{\cup \iota,\text{all-one}}\rangle) + N_{\boldsymbol{F}_i}.
\end{aligned}$$

The $\#\operatorname{cros}(\cdot)$ denotes the total number of crossings. This term appears because the q–degree counts the number of 1–resolutions taken (which will be all of the crossings). The third line breaks this term into several self-explanatory pieces; the $n(n-1)-i$ term handles the crossings "above" the $\boldsymbol{Z}$ (see Figure 5). Meanwhile, the changing of τ' to $\tau + 2n - 6$ in the third line follows from the left-handed version of Lemma 3.5.

From the cofibration (11) above, we see that our goal for the left-handed twists is to ensure that, for all $i = 1, \dots, n(n-1)$ and for all $k \geq b^-$,

$$\begin{aligned} j + (k+1)n(n-1) - (i-1) + N_{\boldsymbol{F}_i} + k\tau_{\boldsymbol{F}_i} \\ > k(n^2 - 3n + \tau_{\boldsymbol{F}_i}) + (n(n-1) - i) \\ + \#\operatorname{cros}(\boldsymbol{Z}) + \#\operatorname{circ}(\langle \boldsymbol{I}_{n-2}, \boldsymbol{Z}^{\cap \iota}_{\cup \iota, \text{all-one}} \rangle) + N_{\boldsymbol{F}_i}. \end{aligned}$$

This is clearly achieved by setting

$$b^- := \max_{\iota = 1, \dots, n-1} \frac{-j + \#\operatorname{cros}(\boldsymbol{Z}) + \#\operatorname{circ}(\langle \boldsymbol{I}_{n-2}, \boldsymbol{Z}^{\cap \iota}_{\cup \iota, \text{all-one}} \rangle)}{2n}, \tag{18}$$

which clearly depends only on j, the number of crossings in $\boldsymbol{Z}$, and the all-one resolution of $\boldsymbol{Z}$ as desired. □

Remark 3.9 Notice the similarity between the bounds b^+ and b^-. In both cases, the bound involves $\pm j/2n$ plus a constant term (independent of j). Thus all of the careful tracking of normalization shifts "cancel out" in precisely the same way regardless of using right- or left-handed twists. The sign change of j versus $-j$ also makes sense when we recall that the graded Euler characteristic of these spaces is meant to give a power series expansion of the corresponding rational functions coming from the Jones–Wenzl projectors, in q for right-handed twists (so using positive j terms) and in q^{-1} for left-handed twists (so using negative j terms). With this in mind, the only real difference between b^+ and b^- comes from the use of the all-zero resolution of D versus the all-one resolution, and the need to count crossings away from the left-handed twists.

We are now ready to prove Theorem 1.4. Let D denote a diagram obtained from a link diagram by formally replacing a finite number of identity braids $\boldsymbol{I}_{n_i}$ with Jones–Wenzl projectors P_{n_i}. Let $m \in \mathbb{N}$ denote the total number of projectors in D. For any $(k_1, \dots, k_m) \in (\mathbb{N} \cup 0)^m$, let $D^{\pm}(k_1, \dots, k_m)$ denote the diagram D with each P_{n_i} replaced by $T_{n_i}^{\pm k_i}$. Note that it is very important that the diagrams have either all right-handed twists, or all left-handed twists. We do not allow any mixing of the two.

We focus on the right-handed case first. Fixing $j \in \mathbb{Z}$, we consider the infinite $m-$dimensional cube of maps built as follows. The vertices of the cube correspond to $(k_1, \dots, k_m) \in (\mathbb{N} \cup 0)^m$. At each such vertex we place the space

$$\mathcal{X}_+^{j+N_D}(k_1, \dots, k_m) := \Sigma^{\sum_{i=1}^m k_i \eta_i} \mathcal{X}^{j+N_D+\sum_{i=1}^m k_i \tau_i}(D(k_1, \dots, k_m)). \tag{19}$$

Here, the subscripts on the normalization shifts τ and η indicate which $\boldsymbol{T}_{n_i}$ is being referred to (see Definition 3.1 and Remark 3.2). Meanwhile, the N_D is referring to the

normalization shift $n^+ - 2n^-$ for all crossings totally separate from any of the inserted twists (ie crossings present in the original diagram D, discounting the Jones–Wenzl projectors). Now between any two adjacent vertices of $(\mathbb{N} \cup 0)^m$, we see all of the k_i remain constant except one of them, say $k_{\hat{\imath}}$, which differs by one between the two vertices. To this edge we assign the map

$$\mathcal{X}_+^{j+N_D}(k_1, \dots, k_{\hat{\imath}}, \dots, k_m) \hookrightarrow \mathcal{X}_+^{j+N_D}(k_1, \dots, k_{\hat{\imath}} + 1, \dots, k_m) \tag{20}$$

induced by Lemma 2.1 as in Proposition 3.7.

Definition 3.10 Given a diagram D involving Jones–Wenzl projectors, define the *(right-handed) Khovanov spectrum of D* to be the wedge sum

$$\mathcal{X}_+(D) := \bigvee_{j \in \boldsymbol{Z}} \mathcal{X}_+^{j+N_D}(D),$$

where for each q–degree $j + N_D$, the spectrum $\mathcal{X}_+^{j+N_D}(D)$ is defined to be the homotopy colimit of the cube of maps described by Equations (19) and (20).

Proof of Theorem 1.4 (right-handed case) We wish to show that the cube of maps defining $\mathcal{X}_+^{j+N_D}(D)$ "stabilizes" in a particular sense. To do this we isolate a single projector $P_{n_{\hat{\imath}}}$ and fix all of the $k_{i \neq \hat{\imath}}$. This allows us to view the maps (20) as (ignoring homological shifts)

$$\mathcal{X}^{j+k_{\hat{\imath}}\tau_{\hat{\imath}}+N_D+\sum_{i\neq\hat{\imath}} k_i\tau_i}(\langle \boldsymbol{T}_{n_{\hat{\imath}}}^{k_{\hat{\imath}}}, \boldsymbol{Z} \rangle) \hookrightarrow \mathcal{X}^{j+(k_{\hat{\imath}}+1)\tau_{\hat{\imath}}+N_D+\sum_{i\neq\hat{\imath}} k_i\tau_i}(\langle \boldsymbol{T}_{n_{\hat{\imath}}}^{k_{\hat{\imath}}+1}, \boldsymbol{Z} \rangle), \tag{21}$$

where the tangle $\boldsymbol{Z}$ includes all of the other $\boldsymbol{T}_{n_i}^{k_i}$. Having fixed j, these maps are all stable homotopy equivalences for $k_{\hat{\imath}} > b_{\hat{\imath}}^+$, for some bound $b_{\hat{\imath}}^+$ that depends only on the all-zero resolution of $\boldsymbol{Z}$. Since the all-zero resolution of any $\boldsymbol{T}_{n_i}^{k_i}$ is just $\boldsymbol{I}_{n_i}$ regardless of k_i, this bound $b_{\hat{\imath}}^+$ is *independent of the other k_i* (this is the point that requires that we do not mix right- and left-handed twists in our construction). Thus we can find the various bounds b_i^+ one projector at a time, effectively ignoring the rest. Since there are only finitely many projectors, we can find a global bound b^+ which works for all of the k_i at once and declare that the cube is stable for all $k_i > b^+$. This also allows us to use simpler notation: let $D(k) := D(k, \dots, k)$, and similarly $\mathcal{X}_+^{j+N_D}(k) = \mathcal{X}_+^{j+N_D}(k, \dots, k)$. Our proof then shows that, for any fixed $j \in \boldsymbol{Z}$, the "diagonal sequence" $\mathcal{X}_+^{j+N(D)}(k)$ stabilizes as $k \to \infty$, and so the hocolim $\mathcal{X}_+^{j+N_D}(D) \simeq \mathcal{X}_+^{j+N_D}(k)$ for some large enough k depending on j. Since the chain complexes of the twists are known to stabilize to the categorified Jones–Wenzl

projectors, the wedge sum $\mathcal{X}_+(D) = \bigvee_{j\in\mathbf{Z}} \mathcal{X}_+^{j+N_D}(D)$ satisfies the requirements of Theorem 1.4. □

The left-handed twists work in exactly the same fashion, so we only mention the slight differences. We populate the vertices of the cube by spaces

$$\begin{aligned}(22)\quad \mathcal{X}_-^{j+N_D}(k_1,\dots,k_m) :=& \\ \Sigma^{\sum_{i=1}^m k_i(\eta_i - n_i(n_i-1))}&\mathcal{X}^{j+\sum_{i=1}^m k_i n_i(n_i-1)+N_D+\sum_{i=1}^m k_i\tau_i}(D(k_1,\dots,k_m))\end{aligned}$$

and the edges are maps

$$(23)\qquad \mathcal{X}_-^{j+N(D)}(k_1,\dots,k_{\widehat{\imath}},\dots,k_m) \twoheadleftarrow \mathcal{X}_-^{j+N_D}(k_1,\dots,k_{\widehat{\imath}}+1,\dots,k_m)$$

induced by Lemma 2.1 once again. Notice the extra grading shift $\sum_{i=1}^m k_i n_i(n_i-1)$, which counts the number of crossings available in all of the $\boldsymbol{T}_{n_i}^{-k_i}$.

Definition 3.11 Given a diagram D involving Jones–Wenzl projectors, define the *(left-handed) Khovanov spectrum of* D as the wedge sum

$$\mathcal{X}_-(D) := \bigvee_{j\in\mathbf{Z}} \mathcal{X}_-^{j+N_D}(D),$$

where for each q–degree $j+N_D$, the spectrum $\mathcal{X}_-^{j+N_D}(D)$ is defined to be the homotopy colimit of the cube of maps described by Equations (22) and (23).

Proof of Theorem 1.4 (left-handed case) Focusing on one projector $(\widehat{\imath})$ at a time as before, the formula (18) for $b_{\widehat{\imath}}^-$ does appear to depend on the other k_i since the term $\#\operatorname{cros}(\boldsymbol{Z})$ will count crossings in the other twists. However, this count is canceled out precisely by the extra grading shift $\sum_{i=1}^m k_i n_i(n_i-1)$, and the bounds b_i^- are again mutually independent allowing the same argument as for the right-handed case to go through. The details here are left to the reader. □

Thus we have two equally eligible candidates, $\mathcal{X}_+(D)$ and $\mathcal{X}_-(D)$, for a spectrum that satisfies the requirements of Theorem 1.4, depending on whether we want to view the Euler characteristic as a power series representation of the corresponding rational function in q^{+1} or q^{-1}. In either case, the wedge summand in a specific q–degree can be computed using a finite-twist approximation $D(k)$, where the amount of twisting k needed depends both on the diagram D and on the q–degree being considered.

Remark 3.12 The independence of the various k_i used in the proofs above has been used to take the homotopy colimit "diagonally", simplifying the notation by tracking only a single value of k. However, this independence can also be viewed as allowing us to take the colimit one projector at a time, in any order we like. This is already implicit in the diagonal version in the passage from $D(k)$ to $D(k+1)$, where it does not matter in what order we treat all of the projectors going from their individual k–twists to their individual $(k+1)$–twists.

3.3 Properties of $\mathcal{X}(D)$

Before going on to establish the connection to spin networks and colored links, we state and prove some properties for $\mathcal{X}_+(D)$ for diagrams D with Jones–Wenzl projectors as above. The propositions in this section will be stated and proved for right-handed twists only; the left-handed versions for $\mathcal{X}_-(D)$ are proved analogously, using alterations similar to those discussed in the previous section. As such, we drop the $+$ notation for the time being.

Our first property is perhaps the most fundamental one. Recall that the first axiom used to characterize both the Jones–Wenzl projectors and their categorifications is that they are "killed by turnbacks". The following proposition gives the analogous statement for our spectra $\mathcal{X}(D)$.

Proposition 3.13 *For any diagram D involving at least one Jones–Wenzl projector that is capped by at least one turnback, $\mathcal{X}(D) \simeq *$.*

Proof Theorem 1.4 ensures that the cohomology of $\mathcal{X}(D)$ matches the homology defined using the categorified Jones–Wenzl projectors, which is known to vanish for such D (see Theorem 2.2). As noted in Remark 1.6, $\mathcal{X}(D)$ has the stable homotopy type of the suspension spectrum of a CW complex up to some finite formal desuspension, and thus Whitehead's theorem implies that the trivial cohomology of $\mathcal{X}(D)$ forces it to be contractible. □

The next proposition ensures that crossings in a diagram involving projectors still give rise to cofibration sequences in the same sense as Equation (4), leading to a version of Lemma 2.1 for our spectra $\mathcal{X}(D)$.

Proposition 3.14 *Let D be a diagram involving a finite number of Jones–Wenzl projectors, and consider a specified crossing in D. Let D' and D'' be the corresponding diagrams where the crossing is replaced with its 1–resolution and 0–resolution respectively. Then we have the cofibration sequence of spectra*

$$\Sigma^a \mathcal{X}^{j+N_{D''}}(D'') \hookrightarrow \mathcal{X}^{j+N_D}(D) \twoheadrightarrow \Sigma^b \mathcal{X}^{j-1+N_{D'}}(D'), \tag{24}$$

where the shifts are precisely the same as those indicated with Equation (4)*. In particular, if either of $\Sigma^a \mathcal{X}^{j+N_{D''}}(D'')$ or $\Sigma^b \mathcal{X}^{j-1+N_{D'}}(D')$ is contractible, then the other is stably homotopy equivalent to $\mathcal{X}^{j+N(D)}(D)$.*

Proof In short, the sequence (24) is built by applying (4) to a suitably large finite-twist approximation $\mathcal{X}(D(k))$ for $\mathcal{X}(D)$. The homological and q–degree shifts coming from (4) are based on counting positive and negative crossings in the honest link diagram $D(k)$. The crossings away from the twists account for the shifts in (24), while the crossings within the twisting contribute only to renormalizing the diagonal sequences used for D' and D''. The final statement is then clear (see Lemma 2.1).

In more detail, we consider the term $\Sigma^{\sum_{i=1}^m k\eta_i} \mathcal{X}^{j+N_D+\sum_{i=1}^m k\tau_i}(D(k))$ in the diagonal sequence used to build $\mathcal{X}^{j+N_D}(D)$ (continuing to use the notation of earlier in this section). Resolving the specified crossing in the diagram $D(k)$ results in the diagrams $D'(k)$ and $D''(k)$ which would be used to approximate $\mathcal{X}(D')$ and $\mathcal{X}(D'')$. The key point to notice is that for the honest link diagram $D(k)$, the shift $N_D + \sum_{i=1}^m k\tau_i$ is the same as $N_{D(k)}$, and similarly for $D'(k)$ and $D''(k)$. Thus we can use Equation (4) to build a cofibration sequence

$$\Sigma^A \Sigma^{\sum k\eta_i} \mathcal{X}^{j+N_{D''(k)}}(D''(k)) \hookrightarrow \Sigma^{\sum k\eta_i} \mathcal{X}^{j+N_{D(k)}} \mathcal{X}(D(k)) \twoheadrightarrow \Sigma^B \Sigma^{\sum k\eta_i} \mathcal{X}^{j-1+N_{D'(k)}}(D'(k)).$$

The homological shifts A and B are differences in total counts of negative crossings. Since a and b account for these differences away from the twisting, the reader can easily verify that $A = a + \sum k(\eta_i'' - \eta_i)$ and $B = b + \sum k(\eta_i' - \eta_i)$. Putting these in place we see the sequence

$$\Sigma^a \Sigma^{\sum k\eta_i''} \mathcal{X}^{j+N_{D''(k)}}(D''(k)) \hookrightarrow \Sigma^{\sum k\eta_i} \mathcal{X}^{j+N_{D(k)}} \mathcal{X}(D(k)) \twoheadrightarrow \Sigma^b \Sigma^{\sum k\eta_i'} \mathcal{X}^{j-1+N_{D'(k)}}(D'(k)).$$

Since all of these spectra stabilize as $k \to \infty$, we can take k large enough so that each term in this sequence is stably homotopy equivalent to the corresponding spectrum in (24). □

Corollary 3.15 *For any diagram D involving an n–strand Jones–Wenzl projector P_n concatenated with a braid β on those n strands,*

$$\mathcal{X}^{j+N_D}(D) \simeq \Sigma^{a+\beta^-}\mathcal{X}^{j+N_{D\setminus\beta}-\beta^-}(D\setminus\beta),$$

where $D\setminus\beta$ is used to denote the diagram created by replacing β with $\boldsymbol{I}_n$, the identity braid on those same n strands (this replacement is referred to as *straightening the braid β*), *and β^- is the number of crossings of the form $\times$ in β viewed vertically (ie the number of crossings that require 1–resolutions to transform β into $\boldsymbol{I}_n$). The homological shift a is the difference between the number of negative crossings in the two diagrams, as in Lemma 2.1.*

Proof Let P_{n_1} be the projector with β concatenated. Since any braid β is a product of elementary generators $\sigma_\iota^{\pm 1}$ in the braid group B_{n_1} (so $\iota\in\{1,\dots,n_1-1\}$), it is enough to prove the statement for such generators (ie for a single crossing above the P_{n_1}). For each $j\in\mathbb{Z}$, Proposition 3.14 allows us to build a cofibration sequence (24) using this crossing. One of the two resolutions will lead to a diagram involving a turnback above P_{n_1}, forcing the corresponding spectrum to be contractible via Proposition 3.13. Thus the other resolution, corresponding to "straightening" the crossing $\sigma_\iota^{\pm 1}$, will give a spectrum stably homotopy equivalent to the original. The $-\beta^-$ shift comes from the -1 term for the 1–resolution in (24) needed to "straighten" any σ_ι^{-1} in β. The homological shift is determined similarly. □

The next corollary can be viewed as lifting the idempotency of the Jones–Wenzl projectors and their categorifications to the realm of spectra.

Corollary 3.16 *Let D be a diagram involving two concatenated projectors of possibly different sizes, say $P_{n_1}\cdot P_{n_2}$ with $n_1\le n_2$* (see Figure 6 for clarification on this notion). *Let D' be obtained from D by replacing the smaller projector P_{n_1} with an identity braid $\boldsymbol{I}_{n_1}$. Then $\mathcal{X}(D)\simeq\mathcal{X}(D')$.*

Proof We fix $j\in\mathbb{Z}$ and replace D by $D(k)$ for $k>b^+$ as in the proof of Theorem 1.4. Here we make stronger use of the independence of the various k_i to fix $k_1>b_1^+$, while still allowing the other k_i to limit towards infinity together. In symbols, we are considering $\mathcal{X}^{j+N(D)+k_1\tau_1+k\sum_{i=2}^m\tau_i}(D(k_1,k,\dots,k))$. Having fixed k_1 in this way, we can view the $\boldsymbol{T}_{n_1}^{k_1}$ as a braid that is allowed to be straightened as in Corollary 3.15.

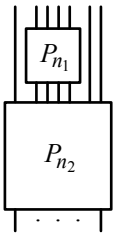

Figure 6: An example of two concatenated projectors $P_{n_1} \cdot P_{n_2}$ with $n_1 \leq n_2$, for which Corollary 3.16 allows us to absorb P_{n_1} into P_{n_2} on the level of the spectra.

When doing this, the grading shift effectively removes the $k_1\tau_1$, and there is no $-\beta^-$ term because all of the crossings are of the form $\times$. This leaves us with precisely

$$\mathcal{X}^{j+N(D)+k_1\tau_1+k\sum_{i=2}^m \tau_i}(D(k_1,k,\dots,k)) \simeq \mathcal{X}^{j+N(D)+k\sum_{i=2}^m \tau_i}(D'(k)),$$

and since the $\boldsymbol{T}_{n_1}^{k_1}$ contributed only full twists to the diagram, the strand orientations before and after the straightening can be the same so that $N(D) = N(D')$. Thus we are left with $\mathcal{X}^{j+N(D')+k\sum_{i=2}^m \tau_i}(D'(k))$, which is precisely the sequence needed to build $\mathcal{X}(D')$. Any homological shifts that are needed along the way cancel precisely; we leave these details to the reader. □

4 Applications to quantum spin networks and colored links

The aim of this section is to provide the necessary background in order to view Theorem 1.1 and Theorem 1.3 as corollaries of Theorem 1.4, and then to prove them accordingly. In short, the "proof" for both statements is that categorified quantum invariants of spin networks and colored links are defined using diagrams involving Jones–Wenzl projectors, for which Theorem 1.4 supplies a well-defined Khovanov spectrum. In the case of colored links, the proof of invariance requires only a few more remarks related to Reidemeister moves and framing. The reader who is already familiar with these subjects can safely skim this section, although the notation used for colored links will be used again in the following sections related to tails. We also state and prove a property about the colored Khovanov spectrum of a 1–colored unknot linking as simply as possible with another colored link related to some discussions in [3].

4.1 Quantum spin networks

A (closed) quantum spin network (the notion dates back to Roger Penrose in [11]) consists of a trivalent graph where each edge has been labeled with a natural number. The labels are not entirely independent: for each vertex where three edges labeled n_1, n_2, n_3 meet, we must have

$$n_i \leq n_j + n_k \quad \text{for all } \{i,j,k\} = \{1,2,3\}, \qquad n_1 + n_2 + n_3 \equiv 0 \bmod 2. \tag{25}$$

From such a spin network G, a q–deformed quantum invariant can be defined as follows (see Chapter 4 in [4]). First we replace each n–labeled edge by a cable of n parallel strands together with a copy of the Jones–Wenzl projector P_n. Then we replace each vertex having edge labels n_1, n_2, n_3 with a "balanced splitting" of the cables as in Figure 7. Call the resulting diagram $D(G)$. The final step is to evaluate the Jones polynomial of $D(G)$, using the rational expressions for the Jones–Wenzl projectors present.

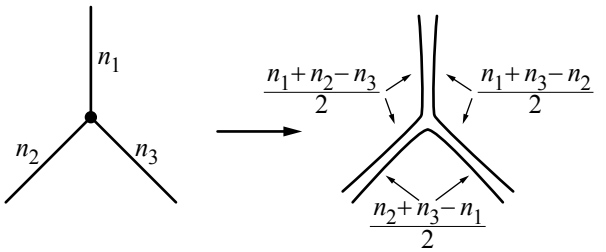

Figure 7: Building the q–deformed invariant of a quantum spin network. The n_i are labels in the original network, and the fractions on the right hand side tell how many parallel strands to send each direction from the vertex.

In [2], Cooper and Krushkal replace the projectors in $D(G)$ with their own categorified projectors, thus defining a categorified spin network. If instead of this we replace the projectors with Rozansky's categorifications using infinite twists, we see a diagram of the form covered by Theorem 1.4.

Definition 4.1 Given a quantum spin network G, we define the *Khovanov spectrum of the spin network* G to be $\mathcal{X}(G) := \mathcal{X}(D(G))$ as defined in Theorem 1.4 for the diagram $D(G)$.

Proof of Theorem 1.3 $\mathcal{X}(G)$ as defined using Theorem 1.4 is clearly well-defined with regards to isotopies of the graph of G, which induce isotopies of $D(G)$. There is

also a "twist" move at a vertex, shown in Figure 8. This move is accomplished by a framing twist on the strand labeled n_1, which would result in a shift of q–degree for the spectrum (a framing twist creates a torus braid on the relevant cable, which can be straightened at the cost of such a shift using Corollary 3.15). This corresponds to the shift described in Section 4.2 of [4]. □

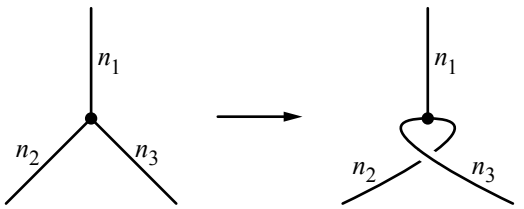

Figure 8: A twist move on a spin network coming from a framing twist on the strand labeled n_1

4.2 Colored links

Let L be a framed, oriented link in S^3 with ℓ components. A coloring of L refers to assigning an irreducible $\mathfrak{sl}_2(\mathbb{C})$ representation to each component of L. Such representations are characterized by their dimension, allowing us to simply consider colorings as assignments of nonnegative integers to each link component (following [12], a coloring of n will indicate the $(n+1)$–dimensional irreducible representation assigned to a link component). That is, for each $h = 1, \dots, \ell$, we color the h^{th} component of L with a natural number n_h. Call such a coloring γ.

Definition 4.2 A *colored link* L_γ is a framed, oriented link L in S^3 together with its coloring γ. The *colored diagram* D_{L_γ} of a colored link L_γ is obtained by taking a blackboard framed link diagram representing L, cabling each component with its designated n_h number of strands (using the blackboard framing), and inserting a copy of the n_h^{th} Jones–Wenzl projector P_{n_h} into each such cabled component. See Figure 9.

Remark 4.3 Note that it is always possible to represent a framed link L by a link diagram where each component is given the blackboard framing. This is accomplished by representing the unframed link L via any suitable projection to the plane as usual, and then adding positive or negative kinks (Reidemeister I moves) to the diagram, which adjust the framing of the link as necessary.

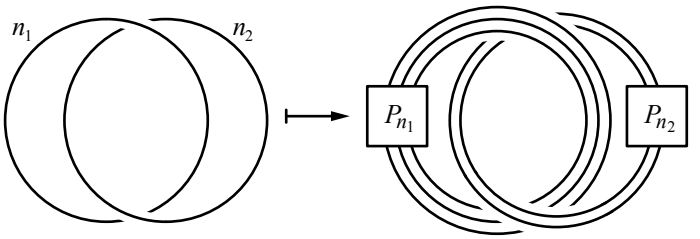

Figure 9: On the left is an example L_γ, with components colored n_1 and n_2; on the right is the colored diagram D_{L_γ} used for calculating the colored Jones polynomial.

Given a colored link L_γ with colored diagram D_{L_γ}, the colored Jones polynomial of L_γ is calculated by taking the usual Jones polynomial of the diagram D_{L_γ}. Using categorified Jones–Wenzl projectors as in [12] or [2], we can build a colored chain complex for L_γ in the same way, whose homology groups are referred to as the colored Khovanov homology of L_γ (see [2] and [13]). Using Rozansky's version of the categorified projectors allows us to prove Theorem 1.1.

Definition 4.4 Given a colored link L_γ, we define the *colored Khovanov spectrum of* L_γ to be $\mathcal{X}_c(L_\gamma) := \mathcal{X}(D_{L_\gamma})$ as defined by Theorem 1.4 for the diagram D_{L_γ}.

Proof of Theorem 1.1 As indicated above, the colored Khovanov homology groups for a colored link L_γ are defined by a link diagram D_{L_γ} involving Jones–Wenzl projectors. Therefore Theorem 1.4 gives the existence of a colored Khovanov spectrum that properly recovers the colored homology. There is a choice of where to place the projector on each cabled component when creating D_{L_γ}. The invariance of $\mathcal{X}_c$ with respect to such a choice is proved one q–degree at a time. Since each $\mathcal{X}_c^j(L_\gamma)$ is equivalent to $\mathcal{X}^j(D_{L_\gamma}(k))$ for some large enough k, and $D_{L_\gamma}(k)$ is just an honest link diagram with $\boldsymbol{T}_{n_h}^k$ in place of the P_{n_h}, we see that these twists $\boldsymbol{T}_{n_h}^k$ can be slid up and down along the cablings, including above or below other cablings, as desired. Similarly, invariance under Reidemeister moves II and III is proved by considering the finite approximation for each j, where such moves give clear isotopies of honest link diagrams. Meanwhile, Reidemeister I moves give framing shifts as expected, since undoing a kink corresponds to adding a full twist on a cable. □

We end this short section with a quick property of the colored Khovanov spectra inspired by the discussion in Section 3.8 of [3], which illustrates the use of Proposition 3.14 and Corollary 3.15 in dealing with the colored spectra.

Definition 4.5 Let L_γ denote a colored link with ℓ components, and let α_h denote the component of L_γ colored with n_h. Define $L_\gamma^{o(h)}$ to be the colored link obtained from L_γ by introducing a new unknotted, 1–colored component $\alpha_{\ell+1}$ that links positively once around the component α_h as in Figure 10.

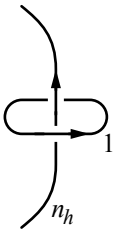

Figure 10: The new unknotted, 1–colored component $\alpha_{\ell+1}$ linking positively once around the component α_h (colored with n_h), forming $L_\gamma^{o(h)}$.

Proposition 4.6 *For any colored link L_γ with ℓ components as above, the colored spectra of L_γ and $L_\gamma^{o(h)}$ for any $h \in \{1, \dots, \ell\}$ fit in the following cofibration sequence:*

$$\mathcal{X}_c^{j+1-2n_h}(L_\gamma) \hookrightarrow \mathcal{X}_c^{j}(L_\gamma^{o(h)}) \twoheadrightarrow \Sigma^{2n_h}\mathcal{X}_c^{j-1-4n_h}(L_\gamma). \tag{26}$$

Proof We focus on $\mathcal{X}_c^j(L_\gamma^{o(h)})$, built via the diagram $D_{L_\gamma^{o(h)}}$. In this diagram we slide the specified P_{n_h} along the cabling to be drawn directly below the "new" unknot $\alpha_{\ell+1}$, which is colored by 1 so that we need no cabling for this component (note that P_1 is just the identity strand). We then construct the cofibration sequence of Proposition 3.14 by resolving the "upper-left" crossing (see Figure 11).

As illustrated in Figure 11, we denote the resulting diagrams D_0 and D_1 for the 0–resolution and 1–resolution respectively. The 0–resolution is also the oriented one, and so the resulting shift in q–degree is only -1 for the loss of a positive crossing. The 1–resolution allows for an orientation as shown in the diagram, where all of the previously positive crossings (there were originally $2n_h$ of them, but one was resolved) become negative. Thus we have a q–degree shift of -1 for the loss of the resolved positive crossing, -1 for the loss of a 1–resolution, and $-3(2n_h-1)$ for the positive crossings becoming negative (-1 each for losing a positive crossing, and -2 each for adding a negative crossing). We also have a homological shift of $-2n_h$ given the loss of a 1–resolution and the addition of $2n_h-1$ negative crossings, which is offset by the $2n_h$ suspension. The diagrams also make it clear that crossings away from this area retain their sign, so that these shifts are the only shifts present and we see

$$\mathcal{X}^{j-1}(D_0) \hookrightarrow \mathcal{X}^{j}(D_{L_\gamma^{o(h)}}) \twoheadrightarrow \Sigma^{2n_h}\mathcal{X}^{j+1-6n_h}(D_1). \tag{27}$$

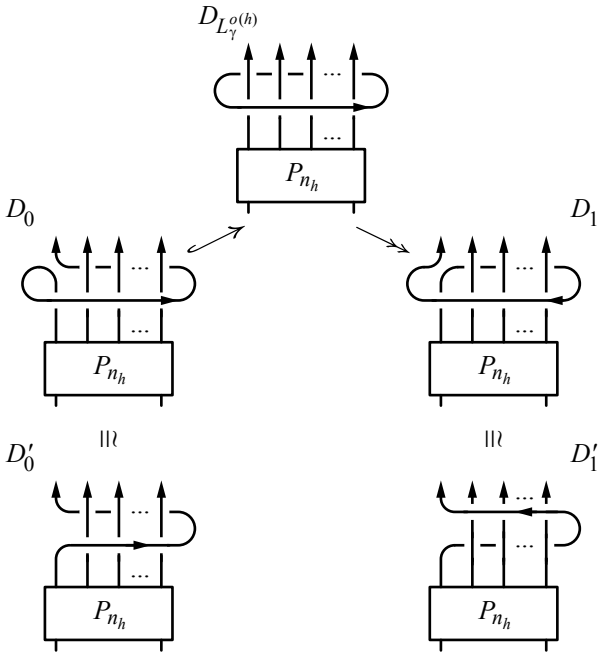

Figure 11: Resolving the upper-left crossing in $D_{L_\gamma^{o(h)}}$ to create a cofibration sequence. The resulting diagrams D_0 and D_1 are isotopic to D_0' and D_1', which allow the use of Corollary 3.15.

At this point, we first use an isotopy (Reidemeister moves) to rearrange D_0 and D_1 into D_0' and D_1' respectively (also shown in the diagram). The D_0' and D_1' are then diagrams with braids above the P_{n_h}. The shifts in (26) are obtained from those in (27) by straightening these braids (all positive crossings for D_0', and all negative for D_1') as in Corollary 3.15. □

Remark 4.7 There are similar cofibration sequences for a (-1)–linking unknot (ie switching the orientation of the unknot $\alpha_{\ell+1}$ in Figures 10 and 11). The details of the resulting degree shifts are left to the reader.

5 Finding a tail for the colored Khovanov homotopy type of B–adequate links

5.1 Discussion and strategy

This section is dedicated to proving Theorem 1.7. Before investigating the details of the proof, we outline the general strategy and logic, expanding on the summary given in the

introduction. The goal is to adapt Rozansky's proof in [13] of the fact that the colored Khovanov homology groups of B–adequate links stabilize as the color goes to infinity. The proof in that paper builds maps f_n that give isomorphisms of colored homology groups between the n–colored and $(n+1)$–colored link L, but only within a certain homological range. In order to prove Theorem 1.7 then, it is enough to show that:

- The maps f_n in [13] are induced by maps F_n between colored spectra, at least within the homological range of isomorphism.
- If n is large enough, the homological range of isomorphism guaranteed by Rozansky is enough to cover all nonzero homology of the corresponding colored spectra (and thus the F_n induce isomorphisms on all homology, and so give stable homotopy equivalences by Whitehead's theorem).

Neither of these statements is difficult to prove conceptually, but the notation involved becomes somewhat cumbersome. The reason is that, on the one hand, the colored spectrum is a homotopy colimit, and in order to build maps we resort to finite approximations (ie the corresponding diagram with high twisting of the cables). This requires q–degree shifts depending on k. On the other hand, the maps f_n built by Rozansky are compositions of a large number of simpler maps, many of which themselves shift the q–degree, which will lead to separate q–degree shifts depending on n. In addition, the maps were built with the use of the categorified Jones–Wenzl projectors rather than finite-twist approximations of them. Thus some care will be needed.

Throughout this section, following [13], all of the twisting will be *left-handed* (ie using $\mathcal{X}_-(D)$ from the proof of Theorem 1.4). We recall here that, in addition to shifts of the form $k\tau$ for the normalization shift n^+-2n^-, the left-handed sequence also requires shifts of the form $kn(n-1)$ for counting the total number of crossings within the twist, accounting for 1–resolutions needed to move backward in the sequence. See Equation (9).

5.2 Notation and a restatement of Theorem 1.7

We begin with some notation. Some of this is repeated from previous sections but is recalled here for convenience. Note that, since the colored Khovanov spectrum of a link requires a specified framing, B–adequacy will be stated in terms of a blackboard framed diagram.

- L denotes a framed, oriented link having a blackboard framed diagram which is B–adequate (the diagram will also be denoted L).

- χ denotes the total number of crossings in the diagram L.
- π denotes the total number of positive crossings in the diagram L (only important for the homological shift, which will be ignored as often as possible).
- $\chi^!$ denotes the total number of crossings in a minimal B–adequate diagram for L, ignoring framing (only important for one key bound).
- ζ denotes the total number of circles present in the all-one resolution of the diagram L.
- $\mathcal{X}_c^j(L_n)$ will denote the colored Khovanov spectrum, in q–degree j, of the link L with all of its components colored with the natural number n; see Definition 4.4.
- For each $(n,k)\in\mathbb{N}^2$, denote by $L(n,k)$ the diagram obtained from L by cabling all components with n parallel strands, and adding a twist of $\boldsymbol{T}_n^{-k}$ to each cabling between *every crossing*. That is, if we replace the diagram L with the graph with vertices at crossings and edges for strands between them, then each edge would be assigned a $\boldsymbol{T}_n^{-k}$ (see the beginning of Section 4 in [13]).
- m denotes the total number of twistings $\boldsymbol{T}_n^{-k}$ coming from Jones–Wenzl projectors in the diagram $L(n,k)$. This plays a similar role to ℓ, the number of components of the link L, in the previous section. However, as the previous item suggests, $m>\ell$ for our diagrams since we will be placing many such twistings on each component.
- For any oriented diagram (link or tangle) D, denote by N_D the normalization shift n^+-2n^- counting all crossings in D.

The following notation is important enough to warrant its own definition.

Definition 5.1 For a given diagram L as above, the *colored q–degree shift* is the integer function $s(n,k)$ that counts the normalization shift, the number of crossings, and the number of circles in the all-one resolution of the link $L(n,k)$. That is, with notation as above,

$$s(n,k) := N_{L(n,k)} + kmn(n-1) + n^2\chi + n\zeta. \tag{28}$$

Remark 5.2 Note that $n\zeta$ is the proper count for the number of circles in the all-one resolution of $L(n,k)$, since each $\boldsymbol{T}_n^{-k}$ present will become an $\boldsymbol{I}_n$, and the all-one resolution of a crossing coming from the original diagram gives a cabled version of the same resolution as in Figure 12.

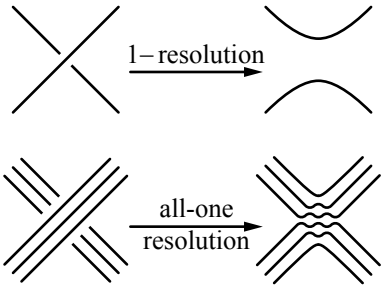

Figure 12: Illustration of the all-one resolution of a crossing in a cabled diagram

Before moving forward, we use this notation to restate the result of Theorem 1.1.

Theorem 5.3 (Theorem 1.1 restated for unicolored links) *For any colored link L_n with the coloring n on every component, there exists a colored Khovanov spectrum $\mathcal{X}_c(L_n) := \bigvee_{j\in\mathbb{Z}} \mathcal{X}_c^{j+s(n,0)}(L_n)$, with wedge summands defined to be the homotopy colimits of the following sequences*

$$\mathcal{X}^{j+s(n,0)}(L(n,0)) \twoheadleftarrow \cdots \twoheadleftarrow \mathcal{X}^{j+s(n,k)}(L(n,k)) \twoheadleftarrow \cdots, \tag{29}$$

which stabilize for large enough k. In particular, for large enough k we have a finite-twist approximation for $\mathcal{X}_c^{j+s(n,0)}(L_n)$ as

$$\mathcal{X}_c^{j+s(n,0)}(L_n) \simeq \mathcal{X}^{j+s(n,k)}(L(n,k)). \tag{30}$$

Remark 5.4 The term $s(n,0)$ is included in the original wedge summand for $\mathcal{X}_c(L_n)$ for convenience moving forward; note that the terms $n^2\chi$ and $n\zeta$ in (28) are independent of k, and simply persist throughout the sequence (29).

Proof This is essentially the sequence built in the proof of Theorem 1.4 for $\mathcal{X}_-(D)$ as applied to Theorem 1.1, except that extra projectors (and thus extra copies of $\boldsymbol{T}_n^{-k}$) are present. These extra projectors cause no issues, however, thanks to Corollary 3.16. In the proof of Theorem 1.4, the shift in the sequence includes a normalization term $-\sum k_i\tau_i$ and a crossing counting term $\sum k_i n_i(n_i-1)$. Here the k_i and n_i are all equal, and both terms are then absorbed into the shift $s(n,k)$. Meanwhile, the left-handed twisting of a cabling where all strands are oriented the same way (in accordance with the orientation of L) means that all of the crossings involved are negative. This ensures that the homological shifts cancel out (we lose negative crossings at the same rate that we lose 1–resolutions), so no suspensions are necessary. □

We now restate Theorem 1.7 in a more precise fashion.

Theorem 5.5 *Fix a framed, oriented B–adequate link with blackboard framed diagram L. With notation as above, for each $j \in \mathbb{Z}$ there exist sequences of maps*

$$\mathcal{X}_c^{j+s(1,0)}(L_1) \twoheadleftarrow \Sigma^{-3\pi}\mathcal{X}_c^{j+s(2,0)}(L_2) \twoheadleftarrow \cdots \Sigma^{-(n^2-1)\pi}\mathcal{X}_c^{j+s(n,0)}(L_n) \twoheadleftarrow \cdots \tag{31}$$

that become stable homotopy equivalences for $n > \chi^! - 2j + 1$.

This version of Theorem 1.7 is the desired final result. However, as indicated in the previous section, we actually build the required maps by taking finite-twist approximations for the various $\mathcal{X}_c(L_n)$. Using (30) we translate Theorem 5.5 into the following:

Theorem 5.6 *Fix a framed, oriented B–adequate link with blackboard framed diagram L. With notation as above, for each $j \in \mathbb{Z}$ and for each $(n,k) \in \mathbb{N}^2$ there exists a map*

$$F_{n,k,j}\colon \Sigma^{-((n+1)^2-1)\pi}\mathcal{X}^{j+s(n+1,k)}(L(n+1,k)) \twoheadrightarrow \Sigma^{-(n^2-1)\pi}\mathcal{X}^{j+s(n,k)}(L(n,k)) \tag{32}$$

such that, for large enough k, the following properties both hold:

(1) *Both the $\mathcal{X}(L(n,k))$ and $\mathcal{X}(L(n+1,k))$ terms are stably homotopy equivalent to their respective colored Khovanov spectra, so that $F_{n,k,j}$ provides the map $F_{n,j}$ below:*

$$\begin{aligned}\Sigma^{-((n+1)^2-1)\pi}\mathcal{X}_c^{j+s(n+1,0)}(L_{n+1}) &\simeq \Sigma^{-((n+1)^2-1)\pi}\mathcal{X}^{j+s(n+1,k)}(L(n+1,k))\\ &\twoheadrightarrow \Sigma^{-(n^2-1)\pi}\mathcal{X}^{j+s(n,k)}(L(n,k))\\ &\simeq \Sigma^{-(n^2-1)\pi}\mathcal{X}_c^{j+s(n,0)}(L_n),\end{aligned} \tag{33}$$

which is used to construct the sequence (31).

(2) *For $n > \chi^! - 2j + 1$, the map $F_{n,k,j}$ (and thus, $F_{n,j}$) is a stable homotopy equivalence.*

Before discussing the proof of this theorem, we provide a table and example to illustrate the statement of Theorem 5.5. The following lemma and corollary are provided to avoid useless clutter.

Lemma 5.7 *For any link L, and for any $n \in \mathbb{N}$, we have that $j = 0$ gives the maximal possible q–degree for nonzero colored spectrum $\mathcal{X}_c^{j+s(n,0)}(L_n)$.*

Proof By the finite-twist approximation (30), we have that

$$\mathcal{X}_c^{j+s(n,0)}(L_n) \simeq \mathcal{X}^{j+s(n,k)}(L(n,k))$$

for some large enough k. The link $L(n,k)$ has Khovanov chain complex generator z with maximal possible q–degree occurring in the all-one resolution, assigning v^+ to all of the circles. Since the all-one resolutions of the left-handed twists give identity braids, this generator z has q–degree equal to

$$\begin{aligned}\deg_q(z) &= \#(1\text{–resolutions}) + (\#(v_+) - \#(v_-)) + (n^+ - 2n^-)\\ &= \#(\text{crossings}) + \#(\text{circles}) + N_{L(n,k)}\\ &= s(n,k),\end{aligned}$$

which corresponds to $j = 0$. □

Corollary 5.8 *For any link L, and for any $n \in \mathbb{N}$, we have that $\mathcal{X}_c^{j+s(n,0)}(L_n)$ is trivial for odd j.*

Proof We see from the proof of Lemma 5.7 that in any finite approximation for $\mathcal{X}_c^{j+s(n,0)}(L_n)$, there is a generator in q–degree corresponding to $j = 0$. The parity of q–degree is constant throughout the Khovanov chain complex, so we must have j even. □

Remark 5.9 Lemma 5.7 can be regarded as giving an alternative meaning for what the grading j, and the shift $s(n,k)$, are describing. We see that $s(n,k)$ is precisely the maximum possible q–grading for the Khovanov chain complex of $L(n,k)$, and then j is a measure of how far from that maximum we are. This means $j \leq 0$, which correctly corresponds to building a power series in q^{-1} for the rational terms in the decategorified setting of the projectors.

We now present the general table of colored spectra for any link L arranged to take advantage of Theorem 5.5.

With Table 1 in mind, we can reinterpret some of the theorems stated above.

- Theorem 5.3 guarantees that all of the colored Khovanov spectra in Table 1 exist, and Equation (30) guarantees that any one of them is stably homotopy equivalent to the

	$j=0$	$j=-2$	$j=-4$	$j=-6$	$\dots$
$\mathcal{X}_c(L_1)$	$\mathcal{X}_c^{s(1,0)}(L_1)$	$\vee\ \mathcal{X}_c^{s(1,0)-2}(L_1)$	$\vee\ \mathcal{X}_c^{s(1,0)-4}(L_1)$	$\vee\ \mathcal{X}_c^{s(1,0)-6}(L_1)\ \vee\ \cdots$	
$\mathcal{X}_c(L_2)$	$\mathcal{X}_c^{s(2,0)}(L_2)$	$\vee\ \mathcal{X}_c^{s(2,0)-2}(L_2)$	$\vee\ \mathcal{X}_c^{s(2,0)-4}(L_2)$	$\vee\ \mathcal{X}_c^{s(2,0)-6}(L_2)\ \vee\ \cdots$	
$\mathcal{X}_c(L_3)$	$\mathcal{X}_c^{s(3,0)}(L_3)$	$\vee\ \mathcal{X}_c^{s(3,0)-2}(L_3)$	$\vee\ \mathcal{X}_c^{s(3,0)-4}(L_3)$	$\vee\ \mathcal{X}_c^{s(3,0)-6}(L_3)\ \vee\ \cdots$	
$\vdots$	$\vdots$	$\vdots$	$\vdots$	$\vdots$	

Table 1: The table of unicolored Khovanov spectra for a link L, with the vertical axis indicating color via subscript on L and the horizontal axis indicating the suitably normalized q–degree. Stabilization occurs vertically starting at a color that depends on both j (the column) and L.

spectrum of a finite-twist approximation $L(n,k)$. Note that there is no single bound for k that approximates all of the spectra in the table at once, since the bound would depend on both j and n.

- Theorem 5.5 asserts that there are "vertical" maps connecting all of the terms in any column of Table 1, and furthermore that these maps are stable homotopy equivalences for $n > \chi^! - 2j + 1$. Thus in any given column (fixed j) we see that the spectra are all stably equivalent for large enough n. This is the general statement of Theorem 1.7.

- Theorem 5.6 is the stepping stone to proving Theorem 5.5. It asserts the existence of the vertical maps *after* replacing each entry in Table 1 by its corresponding finite-twist approximation as guaranteed by Equation (30). Since we build the maps one at a time, we can focus on two adjacent entries in one column of the table (fix j and focus on n and $n+1$ for some n) and take k to be larger than both stability bounds for these two entries. Then this vertical map composes with the finite-twist approximation equivalences as in Equation (33) to give the maps asserted by Theorem 5.5.

To illustrate the stabilization as $n \to \infty$, we build the table for L being the simplest nontrivial link, that is, the positive Hopf link.

Example 5.10 Let L be the positive Hopf link. The reader can quickly verify that

$$\chi = \chi^! = 2, \quad \zeta = 2, \quad N_L = 2,$$
$$s(n,0) = N_{L(n,0)} + 0 + n^2\chi + n\zeta = n^2 N_L + n^2\chi + n\zeta = 4n^2 + 2n,$$

which means that the bound $n > \chi^! - 2j + 1$ for stabilization becomes

$$n > 3 - 2j.$$

Thus we have Table 2 for the Hopf link.

	$j=0$	$j=-2$	$j=-4$	$j=-6$	$\dots$
$\mathcal{X}_c(L_1)$	$\mathcal{X}_c^{6}(L_1)$	$\vee\ \mathcal{X}_c^{4}(L_1)$	$\vee\ \mathcal{X}_c^{2}(L_1)$	$\vee\ \mathcal{X}_c^{0}(L_1)$	
$\mathcal{X}_c(L_2)$	$\mathcal{X}_c^{20}(L_2)$	$\vee\ \mathcal{X}_c^{18}(L_2)$	$\vee\ \mathcal{X}_c^{16}(L_2)$	$\vee\ \mathcal{X}_c^{14}(L_2)$	$\vee\ \cdots$
$\mathcal{X}_c(L_3)$	$\mathcal{X}_c^{42}(L_3)$	$\vee\ \mathcal{X}_c^{40}(L_3)$	$\vee\ \mathcal{X}_c^{38}(L_3)$	$\vee\ \mathcal{X}_c^{36}(L_3)$	$\vee\ \cdots$
$\mathcal{X}_c(L_4)$	$\mathcal{X}_c^{72}(L_4)$	$\vee\ \mathcal{X}_c^{70}(L_4)$	$\vee\ \mathcal{X}_c^{68}(L_4)$	$\vee\ \mathcal{X}_c^{66}(L_4)$	$\vee\ \cdots$
	$\wr$				
$\mathcal{X}_c(L_5)$	$\mathcal{X}_c^{110}(L_5)$	$\vee\ \mathcal{X}_c^{108}(L_5)$	$\vee\ \mathcal{X}_c^{106}(L_5)$	$\vee\ \mathcal{X}_c^{104}(L_5)$	$\vee\ \cdots$
	$\wr$				
$\mathcal{X}_c(L_6)$	$\mathcal{X}_c^{156}(L_6)$	$\vee\ \mathcal{X}_c^{154}(L_6)$	$\vee\ \mathcal{X}_c^{152}(L_6)$	$\vee\ \mathcal{X}_c^{150}(L_6)$	$\vee\ \cdots$
	$\wr$				
$\mathcal{X}_c(L_7)$	$\mathcal{X}_c^{210}(L_7)$	$\vee\ \mathcal{X}_c^{208}(L_7)$	$\vee\ \mathcal{X}_c^{206}(L_7)$	$\vee\ \mathcal{X}_c^{204}(L_7)$	$\vee\ \cdots$
	$\wr$				
$\mathcal{X}_c(L_8)$	$\mathcal{X}_c^{272}(L_8)$	$\vee\ \mathcal{X}_c^{270}(L_8)$	$\vee\ \mathcal{X}_c^{268}(L_8)$	$\vee\ \mathcal{X}_c^{266}(L_8)$	$\vee\ \cdots$
	$\wr$	$\wr$			
$\vdots$	$\vdots$	$\vdots$	$\vdots$	$\vdots$	

Table 2: The table of unicolored Khovanov spectra for the positive Hopf link L. The vertical stable homotopy equivalences begin when $n > 3-2j$, illustrated in the first two columns.

Notice that in the second column of Table 2, stabilization begins after $n = 8$ (that is, $n > 3-2(-2) = 7$). Also, note the absence of horizontal dots in the first row. When $n = 1$, the colored Khovanov homology (and spectrum) is just the usual Khovanov homology (and spectrum), which we know only exists in these four q–degrees for the positive Hopf link L.

5.3 The proof

As mentioned in the discussion on strategy above, the maps $F_{n,k,j}$ will be lifts of the maps f_n defined in Theorem 2.12 of [13]. In that paper, Rozansky considers these as grading-preserving maps between "shifted colored Khovanov homology groups",

$$f_n\colon \widetilde{H}^{i_R,j_R}(L_n) \to \widetilde{H}^{i_R,j_R}(L_{n+1}), \tag{34}$$

where we have used i_R and j_R to denote Rozansky's grading conventions. The existence of these maps is asserted by [13], and the fact that they are isomorphisms so long as $i_R \le n-1$.

Here, we first provide the translation between Rozansky's grading conventions and our own. The reader can verify from [13] that

$$i_R = \#\,\text{cros} - \#\,1\text{–resolutions} = \#\,0\text{–resolutions}, \tag{35}$$

$$j_R = -(\#(v_+) - \#(v_-)) + n\zeta, \tag{36}$$

where the $\#\,\text{cros}$ term refers to the total number of crossings in the diagram D_{L_n} (see Figure 9 in Section 4). From this and Equations (1) and (2) we see that

$$i = -i_R + n^+, \tag{37}$$

$$j = (-i_R - j_R) + (n^+ - 2n^-) + \#\,\text{cros} + n\zeta, \tag{38}$$

where the n^+ and n^- are counting positive and negative crossings in the diagram D_{L_n}. Although some further simplifications are possible, this format most clearly matches the format seen in the sequence (31) of Theorem 5.5 involving the $s(n,k)$ shift.

Now these colored homology groups use the diagrams D_{L_n} containing the categorified Jones–Wenzl projectors. In [12] these categorified projectors are defined as stable limits of complexes using $\boldsymbol{T}_n^{-k}$ in place of the projectors, as in the proof of Theorem 1.1. This means that for large enough k the following homology groups match:

$$\widetilde{H}^{i_R,j_R}(L_n) \cong \widetilde{H}^{i_R,j_R}(D_{L_n}(k)), \quad \widetilde{H}^{i_R,j_R}(L_{n+1}) \cong \widetilde{H}^{i_R,j_R}(D_{L_{n+1}}(k)),$$

so long as $i_R \leq n-1$, the homological range which we are interested in. Thus we may focus on these finite-twist approximations of the colored links L_n, and the maps f_n in this context will give rise to the maps $F_{n,k,j}$ we seek. The reader may check that the grading shifts now correspond to those present in (32).

Now we prove the two lemmas that correspond to the two points discussed in the beginning of this section. For the first lemma, we avoid going into detail about the precise definition of the maps f_n; the interested reader should consult Sections 3 and 4 of [13].

Lemma 5.11 *The maps f_n of Rozansky can be lifted to maps $F_{n,k,j}$ as in* (32).

Proof The maps f_n are built out of several sorts of maps corresponding to local transformations as in Section 4 of [13]:

1. Reidemeister moves involving strands away from the projectors.
2. Short exact sequences of complexes arising from resolving a crossing away from the projectors.

3. "Straightening braids" via resolving crossings adjacent to projectors.
4. Adding new P_n projectors adjacent to an existing P_{n+1} projector, and other similar uses of the idempotent-like behavior of the categorified projectors.
5. "Sliding" projectors above and below other strands.
6. Viewing the categorified P_{n+1} as a cone of a map $C \to \boldsymbol{I}_{n+1}$ where the complex C involves no identity braid diagrams (there are further grading conditions; see both [12] and [13]). This allows a short exact sequence roughly of the form $\mathrm{KC}(\langle C, \boldsymbol{Z}\rangle) \hookrightarrow \mathrm{KC}(\langle P_{n+1}, \boldsymbol{Z}\rangle) \twoheadrightarrow \mathrm{KC}(\langle \boldsymbol{I}_{n+1}, \boldsymbol{Z}\rangle)$.

The first two types of maps clearly extend first to the finite-twist approximations, then to the corresponding spectra (type 1 can be viewed as the content of Section 6 of [7], while type 2 is Lemma 2.1 also based on [7]). Types 3 and 4 lift in a manner corresponding to Corollaries 3.15 and 3.16 respectively, giving stable homotopy equivalences for large enough k. Type 5 is just a combination of Reidemeister moves on the level of the finite-twist approximation, as in the proof of well-definedness of the colored spectrum (proof of Theorem 1.1 in Section 4.2).

For type 6, we return to [12], where the cone format of the categorified P_{n+1} is derived based on the finite-twist approximations, which exhibit this cone structure via resolving all of the crossings in the twisting. And so this map lifts to a long composition of maps of spectra coming from the cofibrations (4) which, on the level of homology, is precisely the desired map.

We note here that some of these maps giving stable homotopy equivalences (especially types 3 and 4) rely not just on Rozansky's bounds, but in the new setting on a proper lower bound for k. Since there are only finitely many such moves used to build the map f_n, we can always force k to be large enough to satisfy all of these lower bounds before we begin. □

The second lemma requires the following theorem from [13].

Theorem 5.12 [13, Theorem 2.1] *Using the notation of Equation* (34)*, we have that* $\widetilde{H}^{i_R, j_R}(L_n) = 0$ *for* $j_R < -\frac{1}{2}(i_R + \chi^!)$.

Proof This is one of several bounds on nonzero shifted colored Khovanov homology provided by Theorem 2.1 in [13]. It is treated as a corollary of Theorem 2.11, which is proved with a spectral sequence built from the multicone presentation of the colored Khovanov chain complex resulting from resolving crossings away from the projectors. See Section 5 of that paper. □

Using this result we can prove the following.

Lemma 5.13 *Fix $j \in \mathbb{Z}$. Then for $n > \chi^! - 2j + 1$, we have (for large enough k)*

$$H^i(\Sigma^{-(n^2-1)\pi}\mathcal{X}^{j+s(n,k)}(L(n,k))) = 0$$

for all $i < \pi - n + 1$, which is equivalent to all $i_R > n - 1$ for $\widetilde{H}^{i_R,j_R}(L_n)$.

Proof For large enough k we have

$$H^i(\Sigma^{-(n^2-1)\pi}\mathcal{X}^{j+s(n,k)}(L(n,k))) \cong H^{i+(n^2-1)\pi}\mathcal{X}_c^{j+s(n,0)}(L_n)) \cong \widetilde{H}^{i_R,j_R}(L_n).$$

Definition 5.1 describes $s(n,k)$ as a count of normalizations, crossings, and circles. This allows us to use equations (2) and (35) to convert

$$\begin{aligned} j + s(n,k) &= j + N_{L(n,k)} + \#\text{crossings}(L(n,k)) + n\zeta \\ &= \#(1\text{–resolutions}) + (\#(v_+) - \#(v_-)) + N_{L(n,k)}, \end{aligned}$$

$$j + \#\,0\text{–resolutions} + n\zeta = (\#(v_+) - \#(v_-)),$$

so that

$$\begin{aligned} j_R &= -\#(v_+ - v_-) + n\zeta \\ &= -j - \#\,0\text{–resolutions} \\ &= -j - i_R. \end{aligned}$$

The last line follows from the fact that the suspensions are designed to ensure that i_R counting 0–resolutions in L_n is the same as counting 0–resolutions in the finite-twist approximation $L(n,k)$. A similar (and simpler) conversion ensures that the bound $i < \pi - n + 1$ is equivalent to $i_R > n - 1$. Meanwhile, the bound $n > \chi^! - 2j + 1$ quickly yields

$$j > \tfrac{1}{2}(\chi^! - n + 1).$$

Combining all of these gives, for $n > \chi^! - 2j + 1$ and $i < \pi - n + 1$ ($i_R > n - 1$),

$$j_R = -j - i_R < -\tfrac{1}{2}(\chi^! - n + 1) - i_R < -\tfrac{1}{2}(\chi^! + i_R),$$

which is precisely the bound of Theorem 5.12 for zero homology as desired. □

Proof of Theorem 5.6 From Lemma 5.11, we have the existence of the required maps $F_{n,k,j}$ that induce isomorphisms on homology for all homological gradings corresponding to $i_R \leq n - 1$. From Lemma 5.13, once $n > \chi^! - 2j + 1$ all of the spaces involved have zero homology in all homological gradings corresponding to $i_R > n - 1$. Therefore for $n > \chi^! - 2j + 1$ the maps $F_{n,k,j}$ induce isomorphisms

on all homology groups, and so by Whitehead's theorem they are stable homotopy equivalences as desired. □

As noted above, this provides the proof of Theorem 1.7.

6 A more explicit tail for the colored Khovanov homotopy type of the unknot

6.1 The idea

In this final section we prove Theorem 1.8 by giving an alternative, more explicit proof showing the tail behavior for the colored Khovanov spectrum of the unknot. Since cabling an unknot with a torus braid twist simply produces the torus links $T(n,m)$, we use the notation $\mathcal{X}(T(n,\infty))$ for the spectrum of the n–colored unknot.

Remark 6.1 There is an important distinction to be made here. Earlier, the notation $\boldsymbol{T}_n^k$ was used to denote a torus *braid* consisting of k *full (right-handed) twists*. Now we use the notation $T(n,m)$ to denote a torus *link* with m *fractional* $1/n^{th}$ *(right-handed) twists* as in [16].

Before going into the details of the proof, we provide a table to illustrate the goal of the construction, similar to Table 1 for the general case. First, a quick lemma that can be regarded as the translation of Lemma 5.7 and Corollary 5.8 into this setting, presented to avoid needless clutter.

Lemma 6.2 *For $n \not\equiv j \bmod 2$, the spectrum $\mathcal{X}^j(T(n,\infty))$ is trivial. Likewise, $\mathcal{X}^j(T(n,\infty))$ is trivial for $j < -n$.*

Proof This is a simple consequence of Corollaries 7.2, 7.3, and 7.4 in [16]. For $n = 2$ and $n = 3$, the statement is clear from the formulas presented there. For $n \geq 4$, one can compute the minimal q–degree available in the all 0–resolution of the relevant torus link (which is just $-n +$ the number of crossings), which gives a minimal q–degree available for $\mathcal{X}^j(T(n,\infty))$ (notice that the degree shift in the formulas of Corollary 7.2 is precisely the number of crossings in the relevant torus link). Since the parity of q–degree is constant throughout the Khovanov chain complex of a given link, the parity of this q–degree can also be used to prove the first statement (after the indices are shifted properly). See Corollary 5.8, or Lemma 7.6 in [16], for a more detailed discussion of this idea. □

	$j=0$	$j=2$	$j=4$	$j=6$	$\dots$
$\mathcal{X}(T(1,\infty))$	$\mathcal{X}^{-1}(T(1,\infty))\ \vee$	$\mathcal{X}^{1}(T(1,\infty))$			
	$\wr$				
$\mathcal{X}(T(2,\infty))$	$\mathcal{X}^{-2}(T(2,\infty))\ \vee$	$\mathcal{X}^{0}(T(2,\infty))\ \vee$	$\mathcal{X}^{2}(T(2,\infty))\ \vee$	$\mathcal{X}^{4}(T(2,\infty))\ \vee$	$\cdots$
	$\wr$	$\wr$			
$\mathcal{X}(T(3,\infty))$	$\mathcal{X}^{-3}(T(3,\infty))\ \vee$	$\mathcal{X}^{-1}(T(3,\infty))\ \vee$	$\mathcal{X}^{1}(T(3,\infty))\ \vee$	$\mathcal{X}^{3}(T(3,\infty))\ \vee$	$\cdots$
	$\wr$	$\wr$			
$\mathcal{X}(T(4,\infty))$	$\mathcal{X}^{-4}(T(4,\infty))\ \vee$	$\mathcal{X}^{-2}(T(4,\infty))\ \vee$	$\mathcal{X}^{0}(T(4,\infty))\ \vee$	$\mathcal{X}^{2}(T(4,\infty))\ \vee$	$\cdots$
	$\wr$	$\wr$	$\wr$		
$\vdots$	$\vdots$	$\vdots$	$\vdots$	$\vdots$	

Table 3: The table of colored Khovanov spectra for the unknots, notated as spectra of torus links, with the horizontal axis indicating suitably normalized q–degree. The vertical stabilizations in each column besides the first begin at $\mathcal{X}^0$, which corresponds to color $n=j$.

With Lemma 6.2 in hand, we can construct Table 3 for the colored unknot.

The goal of this section will be to construct the "vertical" stable homotopy equivalences already presented in Table 3. Note that, like in the general case (Table 1), the j terms are arranged to "start" at zero, but now *increase* in the positive direction. This stems from the fact that we will be using right-handed twists rather than the left-handed twists considered in the previous section. Also, since $T(1,\infty)$ is just an unknot, there is no need for an infinite wedge sum in the first row (similar to the first row in Table 2 for the Hopf link; see Example 5.10).

The construction of these vertical maps follows a simple observation. It is well known that the torus links satisfy $T(n,n{+}1)\cong T(n{+}1,n)$. The sequences used to build $\mathcal{X}(T(n,\infty))$ in [16] were based on going from $\mathcal{X}(T(n,m))\hookrightarrow\mathcal{X}(T(n,m{+}1))$. We can combine these two ideas to see a "diagonal" sequence of the following form (omitting the T from the notation):

$$(39)\quad \begin{array}{lllllll} \mathcal{X}(n,n{-}1)\hookrightarrow\mathcal{X}(n,n)\hookrightarrow & \mathcal{X}(n,n{+}1)\hookrightarrow\cdots & & & \\ & \wr & & & \\ & \mathcal{X}(n{+}1,n)\hookrightarrow & \mathcal{X}(n{+}1,n{+}1)\hookrightarrow & \mathcal{X}(n{+}1,n{+}2)\hookrightarrow\cdots & \\ & & & \wr & \\ & & & \mathcal{X}(n{+}2,n{+}1)\hookrightarrow\cdots & \\ & & & & \ddots \end{array}$$

If we can find a lower bound on n so that all of these maps are stable homotopy equivalences, including the horizontal dots (indicating that in fact $\mathcal{X}(n,n-1) \simeq \mathcal{X}(n,\infty)$, and similarly for the other rows), we would have stable equivalences between spectra $\mathcal{X}(n,\infty)$ as $n \to \infty$, as desired. Of course, this cannot be done once and for all; instead, it is done one (shifting) q–degree at a time. The vertical equivalences in Table 3 will be precisely the resulting maps.

6.2 The proof

The techniques used in this section borrow as much from the results in [16] as from the ideas in this paper. Thus we recall some notation from [16] below.

Definition 6.3 $\mathcal{X}(T(n,\infty)) = \bigvee_{j\in\mathbb{Z}} \mathcal{X}^{j-n}(T(n,\infty))$, where for each $j \in \mathbb{Z}$,

$$\begin{aligned}(40)\quad &\mathcal{X}^{j-n}(T(n,\infty))\\ &:= \operatorname{hocolim}[\mathcal{X}^{j-n}(T(n,0)) \hookrightarrow \cdots \hookrightarrow \mathcal{X}^{(j-n)+m(n-1)}(T(n,m)) \hookrightarrow \cdots].\end{aligned}$$

This is the sequence making up the horizontal maps in the conceptual Equation (39) above. The original definition in [16] did not include the extra q–degree shift of $-n$ in the definition; this term has been included here for convenience, as suggested by the format of Table 3. In fact this shift plays a role similar to that of the term $s(n,0)$ in Section 5. (Indeed, since the unknot has no crossings and one circle in any resolution, this term is precisely $s(n,0)$; the negation is because we will be considering right-handed twisting rather than left-handed.)

In [16] we prove that such sequences of maps become homotopy equivalences for large enough m. We restate the precise result here, as we shall need a small improvement to the bound as well as a careful translation of the q–degrees to our new setting.

Theorem 6.4 [16, Theorem 4.1] *Fix $a \in \mathbb{Z}$ and $n \in \mathbb{N}$. Define*

$$f(a,n) := \max\Big(\frac{a+n-1}{n}, n\Big).$$

Then for any $m \geq f(a,n)$,

$$(41)\qquad \mathcal{X}^{a}(T(n,m)) \hookrightarrow \mathcal{X}^{a+n-1}(T(n,m+1))$$

is a stable homotopy equivalence.

Our new improvement on the bound is very slight, but crucial.

Lemma 6.5 *The bound $f(a,n)$ in Theorem 6.4 can be improved to a new bound*

$$f'(a,n) := \max\Big(\frac{a+n-1}{n}, n-1\Big). \tag{42}$$

The proof of Lemma 6.5 requires one small addition to the proof of Lemma 3.5 in [16], which itself is a result of Stošić. Since this will require reintroducing several notations from [16] that are not used elsewhere in this paper, we relegate this proof to an appendix. Meanwhile, the following corollary translates the result above for use with the sequences (40).

Corollary 6.6 *Fix $j \in \mathbb{Z}$ and $n \in \mathbb{N}$. Then for $m \geq \max(j-1, n-1)$, the sequence* (40) *stabilizes. That is, the maps*

$$\mathcal{X}^{(j-n)+m(n-1)}(T(n,m)) \hookrightarrow \mathcal{X}^{(j-n)+(m+1)(n-1)}(T(n,m+1))$$

are stable homotopy equivalences.

Proof The bound $m \geq n-1$ is the improvement (over $m \geq n$) of Lemma 6.5. Meanwhile, the term $(a+n-1)/n$ in the bound (42) contains the q–degree a, which corresponds here to $(j-n)+m(n-1)$. Some simple algebra ensures that

$$m \geq \frac{a+n-1}{n} \quad \Longleftrightarrow \quad m \geq j-1. \qquad \square$$

With these bounds in place, we are ready to provide the vertical equivalences of Table 3 via the idea of Equation (39).

Lemma 6.7 *Fix $j \in (2\mathbb{N} \cup 0)$. Then for $n \geq j$, we have*

$$\begin{aligned} \mathcal{X}^{j-n}(T(n,\infty)) &\simeq \mathcal{X}^{j-n+(n-1)^2}(T(n,n-1)), \\ \mathcal{X}^{j-(n+1)}(T(n+1,\infty)) &\simeq \mathcal{X}^{j-(n+1)+n^2}(T(n+1,n)). \end{aligned} \tag{43}$$

Proof This follows directly from Corollary 6.6. When $n \geq j$, the $n-1$ term dominates in the bound $m \geq \max(j-1, n-1)$, allowing the sequence (40) to stabilize as soon as $m = n-1$. Of course, if $n \geq j$, then $n+1 \geq j$ as well. $\square$

Lemma 6.8 *For $n \geq j$ as above, define the map $\phi_{n,j}$ to be the composition*

$$\begin{aligned} \mathcal{X}^{j-n+(n-1)^2}(T(n,n-1)) &\to \mathcal{X}^{j-n+(n-1)^2+(n-1)}(T(n,n)) \\ &\to \mathcal{X}^{j-n+(n-1)^2+2(n-1)}(T(n,n+1)) \\ &\simeq \mathcal{X}^{j-(n+1)+n^2}(T(n+1,n)), \end{aligned}$$

where the first two maps are the same maps appearing in the sequence (40)*, and the final equivalence comes from the isotopy* $T(n,m) \cong T(m,n)$*. Then* $\phi_{n,j}$ *defines a stable homotopy equivalence*

$$\phi_{n,j}\colon \mathcal{X}^{j-n+(n-1)^2}(T(n,n-1)) \xrightarrow{\simeq} \mathcal{X}^{j-(n+1)+n^2}(T(n+1,n)).$$

Proof As in the previous lemma, the first two maps are stable homotopy equivalences due to the bound in Corollary 6.6. □

Remark 6.9 We see that this map $\phi_{n,j}$ plays a role similar to that of the $F_{n,j}$ of the previous section, but is much easier to define than the maps f_n in [13] that lead to $F_{n,j}$.

Proof of Theorem 1.8 Combining Lemmas 6.7 and 6.8 gives stable homotopy equivalences

$$\begin{aligned}\mathcal{X}^{j-n}(T(n,\infty)) &\simeq \mathcal{X}^{j-n+(n-1)^2}(T(n,n-1)) \quad \text{(by Lemma 6.7)}\\ &\simeq \mathcal{X}^{j-(n+1)+n^2}(T(n+1,n)) \quad \text{(by Lemma 6.8)}\\ &\simeq \mathcal{X}^{j-(n+1)}(T(n+1,\infty)) \quad \text{(by Lemma 6.7)}\end{aligned}$$

for arbitrary $n \geq j$, which gives all of the necessary stable homotopy equivalences as indicated in Table 3. The calculations presented in Theorem 1.8 refer to the beginning of the stabilization, that is, when $n = j$ so that we are considering $\mathcal{X}^0(T(j,\infty))$. A further application of Corollary 6.6 shows that $\mathcal{X}^0(T(j,\infty)) \simeq \mathcal{X}^{(j-1)^2}(T(j,j-1))$ so long as $j > 0$, while the $j = 0$ case stabilizes immediately (ie for $n = 1$) giving the spectrum of an unknot, which is known to be the sphere spectrum in q–degrees ± 1. □

Remark 6.10 It is clear that a similar argument could be used to define $\mathcal{X}(U_\gamma)$ for an unlink U allowing the colors on each component to tend to infinity. We do not go through the calculation here.

We conclude with a brief discussion on the differences between the new approach of this section and the general approach of the previous one. One difference is that we use right-handed twisting in this new approach, but this is of no consequence and a left-handed version of the new approach could easily be derived. The important difference is that, in the general case, the stable homotopy equivalences required are based on Rozansky's maps f_n, which are very complicated, requiring multiple properties of the categorified projectors (idempotency, straightening adjacent braids, a

careful multi-cone presentation). Even with no crossings (as in the unknot or unlink), the passage from cabling with n strands to cabling with $n+1$ requires extra projectors and clever manipulations between them. In our new approach for the unknot, the only maps required are those that already arise in the stable sequence (40) based on resolving crossings, and maps derived from Reidemeister moves providing the isotopy between $T(n,n{+}1)$ and $T(n{+}1,n)$. In fact this new approach views the tail of the colored Khovanov spectra of the unknot as a stabilization (one q–degree at a time) of the sequence $\mathcal{X}(T(n{+}1,n))$ as $n\to\infty$, rather than as a statement about categorified projectors and colored spectra in the usual sense.

The simple form of the maps used in this approach also gives an improvement on the bound on n for stabilization. In Rozansky's approach, the bound grows like $2j$, while here the bound grows like j. Compare Table 3 to Table 2 to see the gap between beginning of stabilization for adjacent columns in the two cases.

Appendix: Proof of Lemma 6.5

In [16] the bound $m\geq n$ needed for stabilization appears solely due to its presence in Lemma 3.5 in that paper, which itself is a rephrasing of Lemma 1 in [14]. A careful reading of [16] ensures that this bound is never used explicitly again. Thus our goal in this section is to prove this lemma holds in the case $m=n-1$ as well.

For this we recall the notation of [16]. When $m=n-1$, the lemma is concerned with resolving crossings from $T(n,n)$ in order to arrive at $T(n,n{-}1)$. In this situation, we introduce the following notation:

- $D_0 := T(n,n)$.
- For $i=1,\dots,n-1$, the diagrams D_i and E_i are those obtained by resolving the "topmost" crossing of D_{i-1} as a 0–resolution and 1–resolution respectively. Thus we have the cofibration sequences (see [16] for the degree shifts)

$$\mathcal{X}(D_i)\hookrightarrow\mathcal{X}(D_{i-1})\twoheadrightarrow\mathcal{X}(E_i)$$

  and $D_{n-1}=T(n,n-1)$.
- c_i denotes the number of negative crossings present in E_i.

With this notation in place, we wish to prove:

Lemma A.1 *For all* $i = 1, \dots, n-1$,

$$c_i = 2n - 3.$$

Proving this will verify the bound $c_i \geq n + m - 2$ of Lemma 3.5 of [16] in the case $m = n - 1$, and then the rest of the results of [16] go through to prove Lemma 6.5 here.

Remark A.2 Note that these definitions for D_i and E_i are different from those used in the proof of Proposition 3.8, where arbitrary tangles are being considered away from the twisting and we "slide" the topmost twist over to be adjacent to the tangle rather than to the other twists before resolving crossings. The pictures used in the proof below will make the difference clear, and will resemble the similar pictures in [16].

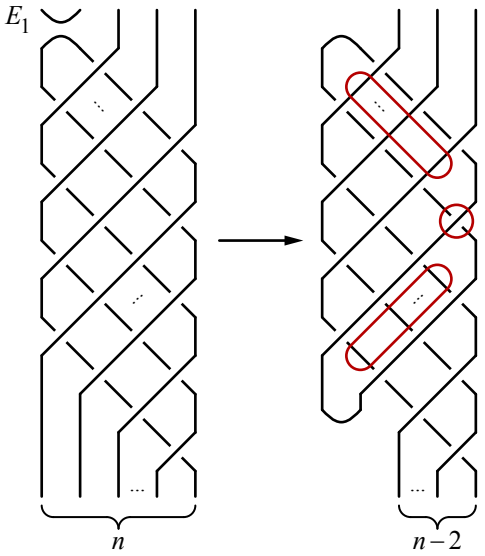

Figure 13: The picture for E_1, where the topmost turnback is pulled around the cabling allowing for the diagram on the right. The red circles in the diagram on the right indicate Reidemeister moves that will occur while pulling the turnback through the twisting.

Proof of Lemma A.1 The case c_1 is considered separately from $c_{i>1}$. For E_1 we see the diagram illustrated in Figure 13, where the strands are closed up outside of the picture in the usual way. The red circles clearly indicate that the turnback can be pulled through via $n-2$ Reidemeister II moves, then a negative Reidemeister I move, then another $n-2$ Reidemeister II moves. Each Reidemeister II move involves precisely one negative crossing, which quickly proves the claim.

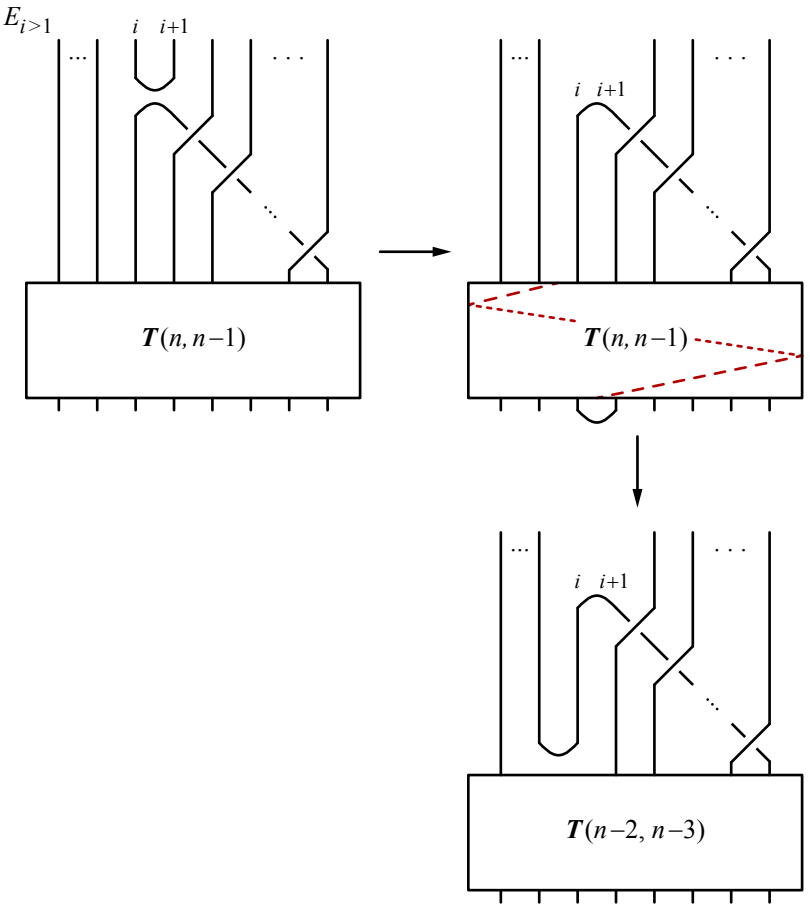

Figure 14: The picture for $E_{i>1}$. The topmost turnback is pulled around the cabling and then through the torus braid $\boldsymbol{T}(n, n{-}1)$ along the indicated dashed line, eliminating two strands from the braid but keeping the twisting at one strand less than a full twist, leaving us with $\boldsymbol{T}(n{-}2, n{-}3)$.

For $E_{i>1}$, we see that the turnback can be pulled through the torus braid $\boldsymbol{T}(n, n{-}1)$ leaving us with a copy of $\boldsymbol{T}(n{-}2, n{-}3)$ as in Figure 14 (note that we use the notation $\boldsymbol{T}$ to indicate the torus braid rather than the complete torus link; however, we continue to use the parentheses notation to indicate fractional twists rather than the full twists indicated by superscripts throughout the rest of the paper).

Now we count crossings similarly to the proof of Lemma 3.5. The initial braid $\boldsymbol{T}(n, n{-}1)$ had $(n{-}1)^2$ crossings, while the new $\boldsymbol{T}(n{-}2, n{-}3)$ has $(n{-}3)^2$ crossings. The crossings "above" the braid remain unchanged, so the total change in the number

of crossings is $(n-1)^2-(n-3)^2 = 4n-8$. Since the turnback was able to swing completely around the entire torus braid (see the red dashed line in Figure 14), it must have accomplished precisely two (negative) Reidemeister I moves. This leaves $4n-10$ crossings eliminated by Reidemeister II moves (see Figure 13 to see that these are the only moves involved). Thus half of the $4n-10$ crossings were negative, plus the two Reidemeister I moves gives precisely $2n-3$ as required. □

References

[1] **D Bar-Natan**, *Khovanov's homology for tangles and cobordisms*, Geom. Topol. 9 (2005) 1443–1499 MR

[2] **B Cooper**, **V Krushkal**, *Categorification of the Jones–Wenzl projectors*, Quantum Topol. 3 (2012) 139–180 MR

[3] **M Hogancamp**, *A polynomial action on colored $\mathfrak{sl}(2)$ link homology*, preprint (2014) arXiv

[4] **L H Kauffman**, **S L Lins**, *Temperley–Lieb recoupling theory and invariants of 3–manifolds*, Annals of Mathematics Studies 134, Princeton Univ. Press (1994) MR

[5] **M Khovanov**, *A categorification of the Jones polynomial*, Duke Math. J. 101 (2000) 359–426 MR

[6] **M Khovanov**, *Categorifications of the colored Jones polynomial*, J. Knot Theory Ramifications 14 (2005) 111–130 MR

[7] **R Lipshitz**, **S Sarkar**, *A Khovanov stable homotopy type*, J. Amer. Math. Soc. 27 (2014) 983–1042 MR

[8] **R Lipshitz**, **S Sarkar**, *A refinement of Rasmussen's S–invariant*, Duke Math. J. 163 (2014) 923–952 MR

[9] **R Lipshitz**, **S Sarkar**, *A Steenrod square on Khovanov homology*, J. Topol. 7 (2014) 817–848 MR

[10] **A Lobb**, **P Orson**, **D Schütz**, *A Khovanov stable homotopy type for colored links*, Algebr. Geom. Topol. 17 (2017) 1261–1281 MR

[11] **R Penrose**, *Applications of negative dimensional tensors*, from "Combinatorial mathematics and its applications" (D J A Welsh, editor), Academic Press, London (1971) 221–244 MR

[12] **L Rozansky**, *An infinite torus braid yields a categorified Jones–Wenzl projector*, Fund. Math. 225 (2014) 305–326 MR

[13] **L Rozansky**, *Khovanov homology of a unicolored B–adequate link has a tail*, Quantum Topol. 5 (2014) 541–579 MR

[14] **M Stošić**, *Homological thickness and stability of torus knots*, Algebr. Geom. Topol. 7 (2007) 261–284 MR

[15] **H Wenzl**, *On sequences of projections*, C. R. Math. Rep. Acad. Sci. Canada 9 (1987) 5–9 MR

[16] **M Willis**, *Stabilization of the Khovanov homotopy type of torus links*, preprint (2015) arXiv

Department of Mathematics, University of Virginia
Charlottesville, VA, United States

msw3ka@virginia.edu

Received: 8 August 2016 Revised: 20 January 2017